INVESTIGATION OF AL_2O_3 PARTICLE REINFORCED COMPOSITE COATINGS ON IF STEEL BY COLD SPRAY

2021
MASTER THESIS
MECHANICAL ENGINEERING

Rajab Hussein Rajab ELKILANI

Thesis Advisors

Assist. Prof. Dr. Harun ÇUĞ

Assist. Prof. Dr. Hüseyin DEMİRTAŞ

INVESTIGATION OF AL_2O_3 PARTICLE REINFORCED COMPOSITE COATINGS ON IF STEEL BY COLD SPRAY

Rajab Hussein Rajab ELKILANI

T.C.
Karabuk University
Institute of Graduate Programs
Department of Mechanical Engineering
Prepared as
Master Thesis

Thesis Advisors
Assist. Prof. Dr. Harun ÇUĞ
Assist. Prof. Dr. Hüseyin DEMİRTAŞ

KARABUK
July 2021

I certify that in my opinion the thesis submitted by Rajab Hussein Rajab ELKILANI titled "INVESTIGATION OF AL_2O_3 PARTICLE REINFORCED COMPOSITE COATINGS ON IF STEEL BY COLD SPRAY" is fully adequate in scope and in quality as a thesis for the degree of Master of Science.

Assist. Prof. Dr. Harun ÇUĞ .....
Thesis Advisor, Department of Mechanical Engineering
Assist. Prof. Dr. Hüseyin DEMİRTAŞ .....
Second Thesis Advisor, Department of Metallurgical and Materials Engineering

This thesis is accepted by the examining committee with a unanimous vote in the Department of Mechanical Engineering as a Master of Science thesis. June 01, 2021

Examining Committee Members (Institutions)	Signature
Chairman : Prof. Dr. Hayrettin AHLATCI (KBU)	.....
Member : Assist. Prof. Dr. Harun ÇUĞ (KBU)	.....
Member : Assist. Prof. Dr. Hüseyin DEMİRTAŞ (KBU)	.....
Member : Assist. Prof. Dr. Özkan ESKİ (KU)	.....
Member : Assoc. Prof. Dr. Yunus TÜREN (KBU)	.....

The degree of Master of Science by the thesis submitted is approved by the Administrative Board of the Institute of Graduate Programs, Karabuk University.

Prof. Dr. Hasan SOLMAZ .....
Director of the Institute of Graduate Programs

"I declare that all the information within this thesis has been gathered and presented in accordance with academic regulations and ethical principles and I have according to the requirements of these regulations and principles cited all those which do not originate in this work as well."

Rajab Hussein Rajab ELKILANI

ABSTRACT

M. Sc. Thesis

INVESTIGATION OF AL_2O_3 PARTICLE REINFORCED COMPOSITE COATINGS ON IF STEEL BY COLD SPRAY

Rajab Hussein Rajab ELKILANI

Karabük University
Institute of Graduate Programs
Department of Mechanical Engineering

Thesis Advisor
Assist. Prof. Dr. Harun ÇUĞ
Assist. Prof. Dr. Hüseyin DEMİRTAŞ
July 2021, 77 pages

In this study, different composite materials were coated on IF-steel by low-pressure cold spray deposit method. Al_2O_3 particle reinforcement was used in all coating materials, and Al, Zn, Ni and Sn powders were used as coating matrix. The effect of coating matrix materials on the coating were investigated by keeping the production parameters constant. The mechanical properties of the coatings were determined by tree point bending, scratch, abrasion, and hardness measurement tests. Micro-level defects and structures were examined by Scanning Electron Microscope (SEM), Energy-Dispersive X-ray (EDX) and Optical analyses. All coatings were applied successfully, and the most significant defects occurred in the Ni-matrix coating. The hardness of the Ni matrix coating was the highest, but the wear resistance was measured in the Zn matrix coating the highest. The lowest hardness and wear resistance were measured in the Sn matrix coating. As a result of the bending test,

distinct crack formations were observed in the Zn matrix coating, unlike the others. All the findings were explained by microstructural studies.

Keywords **:** Cold Spray, Coating, IF-Steel, Wear, Hardness, Scratch Test, Bending Test, Microstructure.

Science Code : 91421

ÖZET

Yüksek Lisans Tezi

AL_2O_3 PARTIKÜL TAKVIYELI KOMPOZIT KAPLAMALARIN IF ÇELIĞI ÜZERINE SOĞUK PÜSKÜRTME ILE INCELENMESI

Rajab Hussein Rajab ELKILANI

Karabük Üniversitesi
Lisansüstü Eğitim Enstitüsü
Makina Mühendisliği Anabilim Dalı

Tez Danışmanı
Dr. Öğr. Üyesi Harun ÇUĞ
Dr. Öğr. Üyesi Hüseyin DEMİRTAŞ
Temmuz 2021, 77 sayfa

Bu çalışmada, IF-çeliği üzerine düşük basınçlı soğuk püskürtme birikimi yöntemi ile farklı malzemeleri kaplanmıştır. Tüm kaplama malzemelerinde partiel takviyesi olarak Al_2O_3 ve kaplama matrisi olarak Al, Zn, Ni ve Sn tozları kullanılmıştır. Üretim parametreleri sabit tutularak kaplama matrisi malzemesinin kaplama üzerindeki etkisi araştırılmıştır. Kaplamaların mekanik özellikleri üç noktadan eğilme, çizilme, aşınma ve sertlik ölçüm testleri ile belirlenmiştir. Mikro düzeydeki kusurlar ve yapılar taramalı elektron mikroskobu (SEM), enerji dağıtıcı röntgen (EDX) ve Optik analizler ile incelenmiştir. Tüm kaplamalar başarıyla uygulanmış ve en önemli kusurlar Ni-matrisli kaplamada meydana gelmiştir. Ni matrisli kaplamanın sertliği en yüksek olurken, aşınma direnci en yüksek Zn matrisli kaplamada ölçülmüştür. En düşük sertlik ve

aşınma direnci Sn matrisli kaplamada diğerlerinden farklı olarak belirgin çatlak oluşumları gözlemlenmiştir. Tüm bulgular mikroyapısal çalışmalarla açıklanmıştır.

Anahtar Kelimeler : Soğuk spray, Kaplama, IF-Çelik , Aşınma, Sertlik, Çizilme Testi, Eğilme Testi, Mikro Yapı.

Bilim Kodu **:** 91421

ACKNOWLEDGMENT

First thanks, God Almighty, and later my father and mother for all their struggles from the day of my birth until this time. You are everything, I love you in God, the most love and I also extend my sincere thanks to my wife who has always been supporting me in all circumstances. Thanks and gratitude to my children, brothers, sisters, and my friends. I am satisfied to thank all those who encouraged, directed and contributed with me through my preparation of this thesis by denoting the needed references and resources in any phase of its phases, and I thank in particular my supervisors Assist Prof. Dr. Harun ÇUĞ and Assist Prof. Dr. Hüseyin DEMIRTAŞ for my support and guiding me with advice and correction and for selecting the title and subject, and my thanks go to the administration of the Faculty of Engineering at the University of Karabuk in the Department of Mechanical Engineering for providing the best environment for teaching engineering sciences in the best conditions for science students.

CONTENTS

Page

Page

Page

LIST OF FIGURES

Page

Page

LIST OF TABLES

Page

SYMBOLS AND ABBREVIATIONS INDEX

SYMBOLS

Al_2O_3 : Aluminum Oxide (Alumina)

SiC : Silicon Carbide

Al : Aluminum

Zn : Zinc

Sn : Tin, (from Latin Stannum)

Si : Silicon

S : Sulfur

Ni : Nickel

Mn : Manganese

Mg : Magnesium

Ti : Titanium

N_2 : Nitrogen

He : Helium

C : Carbon

Cr : Chromium

Cu : Copper

Co : Cobalt

P : Phosphorus

W : Tungsten, (from Latin Wolfram)

Fe : Iron, (from Latin: Ferrum)

Ag : Silver, (from the Latin argentum)

Zr : Zirconium

r : Lankford parameter

Δ_m : Represent the increase in the sample weight during a spray

M_0 : The total material mass, which is thrown at the sample

V_c : Critical Velocity

V_p : Particle Velocity

T_m : Melting point

ρ : Density

R_a : The average surface roughness

R_z : Different of max roughness and min roughness

F_z : Instant normal force

F_x : Tangent force

C_p : Tip dept

ABBREVIATIONS

CS : Cold Spray

(IF) : Interstitial-Free steel

SEM : Scanning Electron Microscope

EDX : Energy-Dispersive X-ray

XRD : X-Ray Diffraction

VPS : Vacuum Plasma Spray

LPPS : Low-Pressure Plasma Spray

HVOF : High-Velocity Oxy-Fuel

D-gun : Detonation gun

ASTM : American Society for Testing and Materials

DE : Deposition Efficiency

FCC : The Face-Centered Cubic

BCC : The Body-Centered Cubic

HCP : The Hexagonal Close-Packed

MMC : Metal–Matrix Composite

PTFE : Poly Tetra Fluoro Ethylene

CoF : Coefficient of Friction

Std.dev : Standard Deviation

PART 1

INTRODUCTION

Steel has become an inextricable part of life specifically in the industrial countries, and it is more significant for the automobile industry. With the industrial expansion of the automotive industry, steel suppliers have to meet stricter demands to produce sheets, which have competitive prices, better gauge tolerance, mechanical uniformity and surface quality. Overall, most industries have a trend towards stronger and lighter steel sheets through down gauging; however, some applications still need formidable steels as their principal requirement. A major and significant formable steel form used for automotive manufacturing is termed as interstitial-free (IF) steels [1]. Due to its outstanding formability, the development of IF-steel has met the need of manufacturers in recent decades. The absence of intermediate atoms, primarily carbon and nitrogen, contributes to the formability of IF-steel [2]. Thus, this form of steels is helpful for manufacturing automobile exteriors (spare wheel well and rear floor pans) and front and rear door interiors [3,4].

Even though IF-steels offer adequate surface characteristics in some applications, they have poor wear and corrosion resistance in general. Protective materials are coated onto IF-steel products, which is an effective and popular method for extending their useful lives. Both Zn and Zn–Al alloys act like corrosion barriers and sacrificial anodes, and they are used as coatings to tolerate high temperature and marine environment [5,6]. Zn and Zn alloys are used in commercial coating, which is performed when the steel products are immersed into molten Zn or Zn-alloy. This process is termed as hot-dipping [7,8]. The mentioned procedures, specifically hot-dipping, are complicated because they are performed at high temperatures. Since the melting bath has a structural limitation, it is difficult to coat large-scale structural workpieces.

Since cold spray is an emerging low-temperature coating process, it makes the deposition of dense and thick coating possible and the process takes place at a rapid rate. This process works using the principle of high-velocity (supersonic) impinging of tiny particles (generally <50μm diameter) on a substrate at a temperature, which is less than the powdered material's melting point [9,10]. Solid particles accelerate to high velocity during the cold spraying process, which is possible because of a high-pressure working gas, which may be air, He, or N_2 that impinges them on the substrate. In this way, the impinged particles form a new surface by deforming on the substrate surface. High-velocity particles have a specific kinetic energy, which is important because deformation, deposition, and impingement processes are dependent on it [11,12]. As a consequence, cold sprays have resolved issues of a thermal spray; so, phase transition, heating, and oxidation effects on a coated material can be avoided [13,14]. Additionally, cold sprays are effective to increase the product lifetime by protecting against corrosion that can be assured through thick coatings.

High thermal conductivities, corrosion resistances, and low densities of aluminum and its alloys make them effective for coating but the mentioned materials have poor tribological performances, and either an appropriate alloy or a matrix reinforcement is needed for applying tough secondary phases, including Al_2O_3 particles [15,16]. In the current circumstances, the importance of tribological behavior of aluminum-based materials is increasing. Most recent research works on composite coating are about nickel coating that consists of carbon fibers and SiC/PTFE particles [17,18]. Furthermore, ceramic coatings, such as Al_2O_3 coating, is also an option because the mentioned coating is abrasive, anticorrosive and heat resistant. Chromium coating is another attractive alternative. It has applications in engine cylinder coatings, coatings needed on dies, high-pressure valves, drill fittings, musical instruments, small aircrafts, electro-technical parts, and car accessories [19]. Consequently, nano-materials, such as nano-composite coatings have become interesting for the researchers, which resulted in large numbers of studies, which have been conducted on nickel coating, its depositing and properties, specifically the one, which consists of Al_2O_3 particles (less than 100nm) [20,21]. Such coatings have unique optical, chemical and mechanical features. To increase the abrasion resistance of micro-devices' metal surfaces, nano- Al_2O_3 coatings are used.

The CS method is generally used with a combination of two comparatively soft and hard powders to promote solid-state deposition. Metal matrix composites (MMC) coatings can be made by using the cold spray technique to combine any hard reinforcing powder with ductile metallic powder. In spite of rapid developments of nanocomposite coatings, there are still some issues pertaining to the nanoparticles' uniform distribution and the coating composition control, which need to be resolved [22,23]. When Al_2O_3 coating is deposited, it results in improved heat resistance, hardness, wear resistance, and anticorrosion properties, which make them functional whenever some kind of aggressive media comes in contact with them [24].

The porosity of sprayed coatings reduction improves their corrosion resistance and sliding wear. We already know that hard ceramic particles (Al_2O_3) can be added to cold-sprayed coatings, which increases their wear resistance, hardness, and coating densities [25], [26]. When the coating density is improved, they can substantially improve their corrosion resistance and sliding wear because their porosity levels are lower. The addition of Al_2O_3 resulted in a decrease in porosity, according to Tao et al. [27]. It also improves adherence by roughening the surface of the pre-applied coating [28]. SiC and Al_2O_3 are the most common ceramic powders utilized as reinforcing particles in cold spraying. SiC and Al_2O_3 are the most common ceramic powders utilized as reinforcing particles in cold spraying. However, Al_2O_3 is more commonly employed in corrosion-resistant technology because it has a better corrosion resistance and chemical stability than SiC [29].

The cold sprayed coatings are currently being developed and their wear and corrosion resistance properties are being investigated. There has not been a thorough investigation of the impact of various matrix composite coatings on if steel. The goal of this research is to investigate the microstructure and wear resistance of X– Al_2O_3 (X=Al, Sn, Zn, Ni) composite coatings on IF steel substrates using a cold spray deposit method. The impact of matrix material on coating bond strength, hardness and wear resistance has been investigated using three different lattice materials (Al-FCC, Ni-FCC, Zn-HCP and Sn-BCT).

PART 2

INTERSTITIAL-FREE (IF) STEELS

2.1. INTRODUCTION

Steel sheets are considered as an important form of structural material while the primary consumer of cold rolled sheet is the automotive industry; therefore, the sheet steel requirement as a structural material in the automobile industry has driven the manufacturers to improve the sheet formability. Steel sheets presently account for roughly half to two-thirds of the total steel material used in an average automobile [30,31]. The need for steel sheet with excellent functional properties, including improved formability, shape stability (little elastic spring back), good surface appearance, weldability, energy absorption, corrosion resistance, and fatigue strength, has been intensified by direct competition with lightweight aluminum alloys and reinforced plastics [32].

The ability to produce complex shapes in a reduced number of stampings with increased strength for reducing the overall vehicle weight requires a great deal of research and studies of the variables that influence their formation and post-formation properties. The main parameters that influence the cold formability of steel sheet are linked with 1) intrinsic material properties, 2) microstructures determined by the thermo-mechanical processing and the strain path, 3) tool geometry and lubrication, 4) local and global stress states, and 5) heterogeneities, such as surface defects or irregularities. These factors are not independent; for instance, damage by growth and coalescence of voids, which depends on the second-phase particle size and distribution, which is a function of the stress state and strain path. These in turn are influenced by the interaction between the lubrication, tools, and the workpiece [31,33].

Removing carbon and nitrogen (interstitial elements) from ferrous solid solution, improves the response needed for severe forming operations. This approach has developed IF-steels, to which, titanium and/or niobium are added to form carbides and nitrides with the help of interstitial carbon and nitrogen atoms. IF-steels were first patented in 1970s by Armco Steel Corporation (now AK Steel) but the company did not initiate large-scale commercial production until the developments in vacuum degassing and continuous annealing technologies. Presently, ultra-low carbon (ULCs) steels, which have less than 50 per million carbon particles, are used to make IF-steel sheets [34], but the same technology is applied to develop high-strength (HS) IF-steels, stainless IF-steel, and bake-hardening steels. The ULC IF-steels have extraordinary cold formability and resistance to strain ageing; therefore, they are mainly used for automotive applications, which require excellent formability and stringent quality control [35].

2.2. HISTORICAL BACKGROUND

Conventional cold-forming steel is at the lower end of the carbon concentration range, so it is a mild steel that is highly ductile. After continuous developments, it parallels micro-alloyed steels because their carbon and nitrogen content is reduced (both the substances impair the steel formability); so now, it has compatibility with postmodern steel processing, making, fabrication, and finishing. Micro-alloys play a significant role in this context but primarily, they are added for different reasons. Basically, they strongly combine with both nitrogen and carbon and help increasing the sheet strength. Since 1930s, titanium and niobium are used for scavenging interstitial nitrogen as well as carbon in different stainless steels for preventing their combinations with chromium that ultimately leads to a welding decay [36]. It is termed as “stabilization”. Similarly, they are also used for stabilizing low-carbon IF-steels [37], but practically, this approach became popular in the 1980s [37] soon after the time when producing ultra-low-carbon content steels (< 0.005%) became possible. The mentioned low-carbon steels were now cementite-free and they have almost 100% ferritic microstructures. They display deep drawing behavior, and besides, they can be hot-dip galvanized and continuously annealed. Still, their formability can possibly be low because of either carbon or nitrogen contents; so, niobium and titanium are added for eliminating their

residual quantities, which forms stable TiN/NbC in ferrite despite the fact that some recent studies claimed that sulfur might help through formation of $Ti_4C_2S_2$ and TiS [38]; so, in this case, Ti captures carbon. Now, these ultra-low-carbon (ULC) steels are termed as IF-steels, which are widely applied for cold-press operations [1].

2.3. CHEMICAL COMPOSITION AND MECHANICAL PROPERTIES

IF-steels are highly-formable with strain hardening exponent $n \geq 0.22$ and Lankford parameter $rm \geq 1.8$, so they are used in white goods and automotive sectors [1,39]. After several steelmaking process advancements, it is now possible to minimize interstitial elements (total $N \leq 40$ ppm and total $C \leq 30$ ppm) in IF-steels during the past few decades [37,40]. Stabilizing elements are again added to the remaining interstitials, which include Nb and/or Ti that form different nitrides, carbides, carbo-nitrides, carbo-sulfides, and sulfides [40,41]. The process of precipitation transforms the ferritic matrix into "interstitial free" that stops the ageing process. Although IF-steels are helpful to the automotive industry because they meet the stringent formability requirements; however, their major drawback is their low strength (yield strength ≤ 200 MPa and tensile strength ≤ 360 MPa). It has partially resolved the issue by applying different metallurgic procedures. P, Mn and Si are some substitutional elements, which are added to IF-steels for transforming them into stronger IF-HS steels [39]. Excessive carbon content in solid solution leads to dislocation hardening, which might develop bake-hardened (BH) and dent-resistant IF-steels [42]. During cold rolling, grain refinement (through heavy deformation or Nb) strengthens IF steels to a certain extent [43]. In spite of all the available processes, which are mentioned so far, the IF-steels' maximum achievable tensile strength is as low as 450 MPa that is lower than the strengths of auto-grade steels, including transformation-induced plasticity (TRIP), multi-phase (MP), and dual phase (DP) steels [44]. The SEM micrograph of a conventional IF-steel is shown in Figure 2.1. It has a low volume fraction of precipitates and most inclusions are cubical TiN crystals with approximately 1μm edge lengths on average.

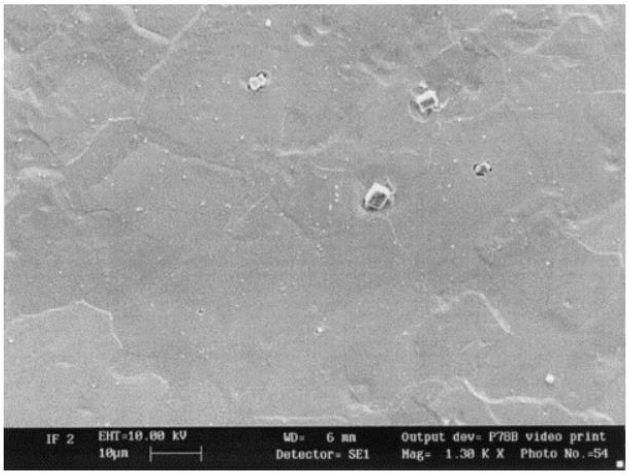

Figure 2.1. IF steel surface in a SEM micrograph that shows the cubical shape of TiN precipitates [45].

Employing the potential strain ageing behavior is an alternative route to increasing strength in IF-steels. When steel has a continuous yielding condition after cold pressing, in that case, it is annealed at a specific temperature. This temperature helps decoration of dislocations through movement of free interstitial atoms, and the formed component achieves significant strength. Annealing is possible through paint curing/baking that is accomplished at a 140–2008 °C. It improves the finished press formed dent resistance of sheets, which is also called bake hardening [37]. Since IF-steel sheets are normally produced through continuous or batch annealing, which exhibits strong texture and thus, it has excellent deep draw-ability. Such steels have been developed rapidly and they have been used for automotive manufacturing and allied industries [41].

Since the interstitial carbon has no solid-solution strengthening effect, the produced steels are soft (<200 MPa yield strength). In this case, strength can be improved using substitutional solid-solution hardening. Other than small Mn and Si additions, phosphorus is used that is a substitute solid-solution strengthener for iron (10 MPa per 0.01% P), which leads to emergence of rephosphorized steel grades for autobody strip that have 220–260 MPa yield strengths. With free carbon/nitrogen levels, a concerning autobody steel group is under-stabilized that is controlled at almost 0.001%. When paint baking is performed, ageing of a cold-formed component takes place at almost 1708 °C, and it implies that carbon/nitrogen diffusion towards the dislocation pins

them. It has almost 50 MPa effect on the strength that raises the dent resistance, which makes them bake-hardened steels with approximately 250 MPa yield strength [37].

The most reliable test for mechanical characterization IF-steels is the strip tension test that predicts failure through two bifurcations in the strain field, which are termed as localized and diffused necking. The stress and strain fields are homogeneous up to the point of uniform elongation in the whole specimen. Both thickness and width in the mid-part of the specimen squeeze after this point (diffuse necking). Later, deformation becomes concentrated in a small band with almost 55° inclination in the direction of loading. In the direction of thickness, the band almost entirely thins out (also called localized necking/shear banding) and finally ruptures. In a strip tension test, this type of instabilities are depicted as failure macro-mechanisms. We can observe void nucleation, coalescence and growth on the microscale. They are common ductile failure micro-mechanisms. SEM micrograph (Figure 2. 2) shows the fracture surface which shows dimples and micro-mechanism of a ductile fracture (growth, coalescence and void nucleation). On the bottom of the dimples, precipitates are visible that cause void nucleation [45].

Lankford parameter is the most significant parameter for automotive body application. It can be measured as a ratio of the strain in the width direction to the strain in the thickness direction that can be obtained applying a simple tensile test. The deep draw-ability of a material is measured through the r-value. A high r-value means deep draw-ability. Higher r-value needs a strong rolling plane formation (denoted by c or ND fibre). So far, high r-values have been observed in IF steels [40]. Engineering properties and the chemical composition of the studied steel EN 10130 DC05 are given in Table 2.1. EN 10130 DC05 is a non-ageing and low-carbon steel, which is especially suitable for deep drawing and for particular applications, such as automotive components and body panels, building materials, and domestic appliances [46].

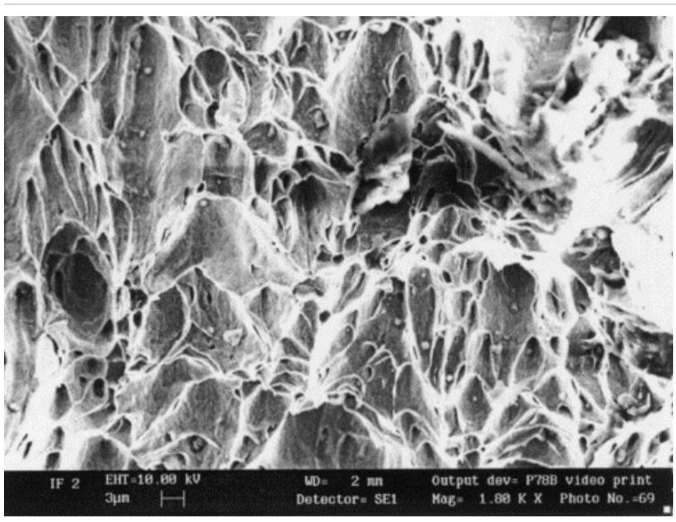

Figure 2.2. Fracture surface of an IF-steel through a SEM micrograph [45].

Table 2.1. Hardness value and chemical composition of DC05 [46].

Vickers Hardness max	Chemical Coposition			
	C % max	P % max	S % max	Mn % max
100	0.06	0.025	0.025	0.35

2.4 ADVANTAGES AND LIMITATIONS

IF-steel belongs to the group of deep drawing steels, and it is a third generation steel, which is used for automobile manufacturing besides Al-killed steel because of its excellent deep draw-ability, high elongation (El), high plastic strain ratio, low yield-to-tensile strength (TS) ratio, and high hardening index. Such advantages remarkably improve its applications for automobile industry specifically in sheet stamping [47,48].

IF-steels are growing in demand specifically for manufacturing, which is obvious from the substantial rise in the IF-steels' production ratio. They are attractive because of their non-ageing behavior and good ductility but the most significant element, which makes them so popular, is their deep draw-ability. They are specifically useful for galvannealed and hot-dip galvanized applications because of ultra-low carbon. IF-steel is better than A1 killed low-carbon steel because it ages slowly and it is deep draw-

able. Different constraints exist in the IF-steel production, such as expensive alloying additions, need for a vacuum degassing installation, and high-finishing rolling temperature [49].

Although interstitial-free sheet steels exhibit excellent cold formability, the occurrence of a brittle fracture can limit their usefulness. Brittle fracture is primarily intergranular in character and it competes the plastic flow during the primary or secondary forming operations or during the in-service use [31]. It is known by different terms, such as secondary work embrittlement (SWE), cold work embrittlement (CWE), longitudinal cracking, or strain induced embrittlement [50]. The cracks usually propagate in the drawing direction. Interstitial-free steels are especially susceptible to intergranular fracture, as there is interstitial free carbon in the solid solution left to segregate to the grain boundaries, where it competes for sites at the grain boundary with impure elements (or directly repel impure atoms) and/or directly strengthen the grain boundary [50]. In the absence of free carbon, grain boundary segregation of impurities or alloying elements, such as P, Sn, Si, S, and As (especially group IVB to VIB elements) is increased, which further weakens the grain boundaries. The lack of carbon and increased segregated impure elements at the grain boundaries are coupled with increase in the flow stress. Intergranular fracture might also form in the direction of the prior compressive strain.

If we look at the IF-steel microstructure, it is a single-phase ferritic microstructure that has low interstitial nitrogen and carbon, and it leads to low strength because of interstitial atoms, which have a lower solid solution hardening effect [51,52]. Additionally, IF-steels' low strength limits its long term and broad application in situations, which require high strength and significant formability levels. Adequate ductility enhances the strength that may raise the potential applications of IF-steel sheets in certain defense or aviation industries [53].

2.5. STRIP STEEL IN AUTOMOTIVE APPLICATIONS

The formability of steel sheets that enables a material's formability in a specific shape is important for producing complex components using sheet metal. Different factors

like die and punch geometry, metallurgic and mechanical properties, sheet thickness, lubrication, punch speed, and sheet roughness. All of them contribute towards the stamping success/failure [4]. In this case, the sheet metal formability should be good enough for manufacturing high-quality stampings. For vehicle design, sheet metal is a critical factor because it has impressive design versatility. In consumer industries, low-carbon sheet steel is a workhorse material that can be stamped into complex and inexpensive components at a high production rate. In several non-ferrous alloys, there is a continuous trend towards material development that has higher formability that results in deep and extra-deep drawing quality [4,54].

In the last few years, IF-steel development has successfully met the car manufacturers' demand because of its excellent deep draw-ability and high value. During the recent development of the automobile industry, the component design of car panels is now more complex and different car panel parts are punched at the same time. The steel sheets now have better deep drawing properties because of new technology, and it came in the limelight when car manufacturers and material researchers extensively studied it. It is a fact that room-temperature sheet metal is extensively used in the car industry for fabricating different body parts, which are drawn despite complex geometries. IF-steel is now a reliable material, which meets the operational needs of the forming operations for two reasons: high planar isotropy and excellent formability [53,55].

PART 3

SURFACE TREATMENT

3.1. INTRODUCTION

The life of a machine component mainly depends on the wear of in-service components. Wear-driven failures normally damage the metal parts, which results in functionality and dimensional losses. For reducing wear, a repair worker normally has two options: Either use a new component made of wear-resistant material or add alloying materials or surface treatments to improve the material's wear resistance. Sometimes, changing the properties of a raw material becomes too challenging. In that case, surface coating improves the material durability and performance, specifically for the components, which continuously expose to extreme working conditions or aggressive environments. In that case, several coatings are applied using multiple coating techniques [56].

Wire-arc, plasma, flame and high-velocity oxy-fuel (HVOF) sprays are common thermal spraying processes, which significantly protect steel corrosion and wear but excessive spray powder oxidation, when a spray is done, increases the oxide content in the coating, which increases the overall oxidation levels and deteriorates the corrosion resistance.

The new cold spray process is an impressive alternative to fabricating alloys because it does not need high temperature for melting powdered particles; so, different hazardous effects, including phase transformation, oxidation, and decomposition can be either eliminated or minimized. The mentioned effects are inherent in the traditional thermal spray processes. Deposits of cold spray are spread through spray particles' plastic deformation [57,58].

3.2. BEGINNINGS OF COLD SPRAY PROCESS

A NASA report mentioned that during takeoff/landing, flying insects come in contact with an aircraft's wings. The little blasts of bugs against the airplane's wings disrupt the laminar air flow, which leads to excessive fuel consumption because it creates more drag in the airplane; therefore, a NASA "bug team" conducted different flight tests to decrease the bug contamination on the commercial aircraft wings [59].

In order to assure optimal aerospace design and safety procedures, Russian scientists studied the impact of particles on flow structure and conducted wind tunnel experiments on the particles' interaction with a body. The mentioned experiments were conducted during the mid-1980s at the Russian Academy of Science (RAS), which is located in Novosibirsk [60]. This led to wind tunnel experiments at RAS, which resulted in observing the deposition of aluminum for the first time on a "cold" (280°K) body with a supersonic two-phase flow that has an aluminum particle moving at 400–450m/s [61].

After the "happy accident" of observation, the cold spray process was developed by some scientists, including Dr. Papyrin, who deposited several pure metals, composites, and alloys onto many substrates, which makes the cold spray process a feasible method. In 1994, a US patent was issued, which was followed by a European patent in 1995. Despite the fact that the cold spray procedure is around for several decades, its commercial development began in 2000s [62]. After that, exponential growth has been observed in the research publications on cold spraying that further increased "patent race" on this process.

3.3. ADVANTAGES OF COLD SPRAY

Like any other material consolidation technique, cold spray has its own benefits and limitations because in fact, it is a solid-state process, which leads to different outcomes. The most obvious limitation is the inherent plastic particle deformation, which decreases ductility but also reduces strength. Strength may be a benefit for certain applications. Additionally, they have many interlinked properties, such as high

density, no oxidation, and low porosity, which are interlinked and they reduce thermal as well as electrical conductivity.

Moreover, cold spray is now extensively used for remanufacturing because it helps manufacturers by reducing negative environmental effects during urgencies, such as resource overexploitation, waste disposal, contamination and greenhouse gasses. This technology is an environment-friendly option as compared to its alternatives, such as painting, electroplating, and soldering. The advantages of cold spray are given in Figure 3.1.

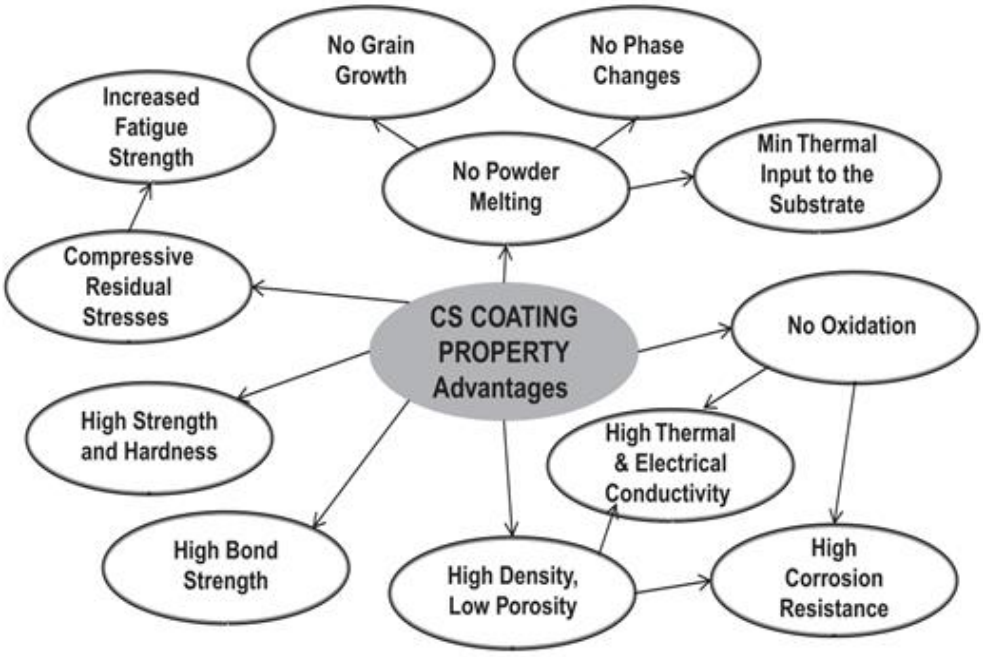

Figure 3.1. Property advantages of cold spray coating [59].

3.3.1. Melting Without Powder

Material consolidation takes place as a consequence of cold spray in a solid state, which is a major difference between conventional thermal spray and cold spray [61]. For stimulating bonding through a quick plastic deformation, it needs sufficient impact energy (particle velocity). Preheating is applied to the compressed gas to assure higher gas flow velocities in the DeLaval nozzle but in case of higher preheating temperatures (1000°C or more), there is a very short contact time for the spray particles, and the gas

cools down, which expands the nozzle's diverging section while it has a remarkably low actual particle temperature as compared to the spray material's melting temperature and the preheating temperature [63].

3.3.2. No Grain Growth

When other materials' consolidation is in progress, like the powder metallurgy or thermal spray processes, recrystallization or grain coarsening takes place, which is unacceptable in some applications [59]. Contrary to that, when cold spraying is initiated, the input heat is kept sufficiently low so as to avoid extensive grain recrystallization and growth. It is specifically helpful because it helps retaining physical and mechanical properties of a consolidated material [64], which include fatigue strength that depends on the grain size and surface microstructure. When a cold-spray is accomplished, the microstructure of a consolidated material grain remains equaxial, which is contrary to the conventional thermal sprays, and it results in a splat-like microstructure [59]. Some authors claimed that fine grain microstructures, which have higher hardness and ultimate tensile strength, have better properties, which can be observed, and besides, high plastic deformation level is common in a cold spray procedure [64,65]. During cold spray, rapid plastic deformation takes place at a more microstructural level, which may form grain zones of nano-size at the interfacial regions that has mechanical implications of deposits of a cold spray [59]. Consequently, the cold spray technique has low-temperature solid-state conditions, which makes it useful to process temperature-sensitive substances, including amorphous and nanostructured materials [65,66].

3.3.3. No Phase Changes

The chemical, microstructural and phase compositions affect the properties of all materials. Mostly, such properties are engineered using processing techniques, which involve high-temperature phase transformations. For high-temperature procedures like plasma spray, molten (including ceramic) species react when they take a very short spray gun-to-substrate flight. For instance, all possible phases are obvious in NiAl plasma-spray powder. It happens for Ni, NiAl, alpha-Ni, $NiAl_3$, Ni_2Al_3, and Al, TiO_2,

and Al_2O_3, which are plasma-spray powder blends. They resulted in significant Al_2O_3 deposition, which are enriched using TiO_2 [59]. When low-temperature spray processes were initiated, the WC–Co and HVOF powders show a tendency to go through detrimental decarburization, when the reactionary by-products are undesirable, including WO_3, W_2C, and W [59], [66]. In cold sprays, thermal phase transformations are avoided. Many researches involve cold sprays for consolidating WC-based powders. Using X-ray diffraction (XRD), it was observed that in grain structure, chemical properties, and phase composition, no change takes place [64,66,67]. It is another classical example regarding nano-crystalline microstructure preservation that shows exceptional mechanical properties, as Figure 3.3 shows [67]. For consolidation, nanostructured powder materials are useful because they do not affect the fine grain size [65].

3.3.4. Minimum Thermal Input to the Substrate

To repair an affected ion vapor deposition (IVD), high-strength steel substrates (4340, 4130, or 300M) are quoted with aluminum, which require more than 99 wt.% aluminum coatings, and they do not increase the substrate temperature above 204 °C (MIL-DTL-83488D). Cold spray technology is ideal to repair thin plates of damaged IVD aluminum because of its low-temperature deposition.

According to qualification tests on cold spray coating, the steel sheets' reverse side temperature (1mm thin) was not more than 120°C [68]. Other than IVD, damaged sputter aluminum, ionic liquid aluminum coatings, and chemical vapor deposition (CVD) can be repaired using cold press [68]. It can also be used to process sensitive substances like magnesium, nanostructured materials, carbide composites, polymers and amorphous materials. Experts believe that this technology is applicable to about 70% materials [59].

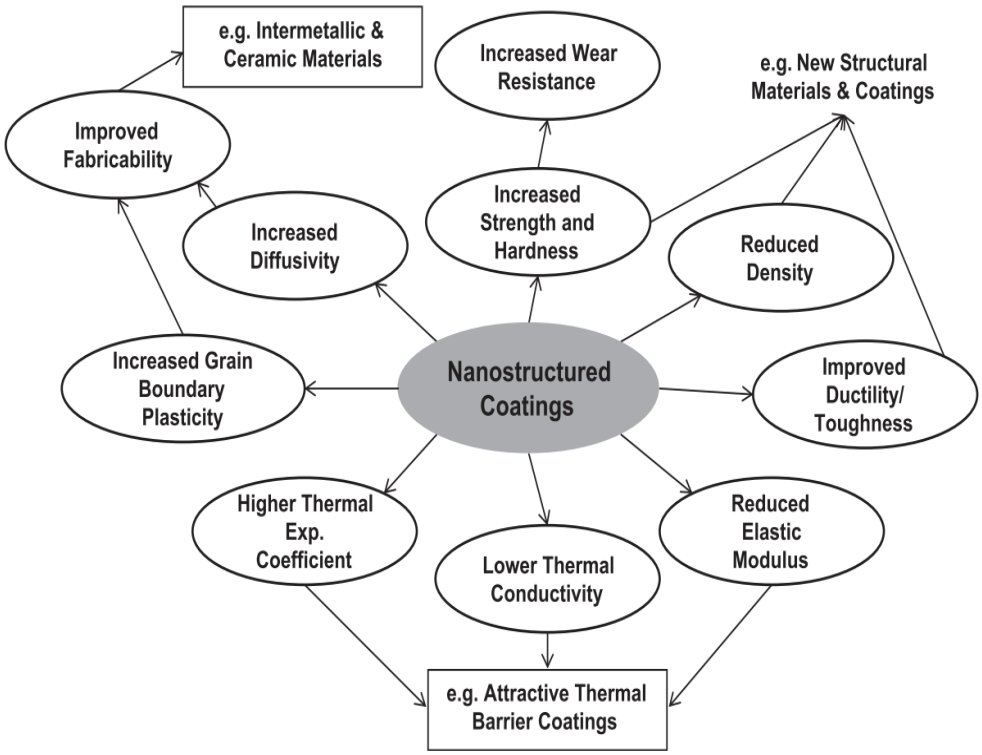

Figure 3.2. Cold spray nanostructured coating advantages [67].

3.3.5. No Oxidation

A major limitation of the most traditional thermal spray procedures is the in-process oxidation. The in-flight particle oxidation adds internal oxide whereas the post-impact oxidation results in formation of oxide layer among splat layers [69]. Air plasma and wire-arc sprays are low-cost processes, which result in most oxidation and porosity in the coatings as compared to HVOF [69]. In HVOF, the increased particle velocity normally correlates with less porosity and improved splat deformation but it is unfortunate that it has no impact on oxidation [59]. Particularly, oxidation becomes critical when oxygen-sensitive substances are sprayed, like copper, aluminum, titanium, and magnesium because small but undesirable oxygen quantities can degrade their physical properties [67]. Nickle-based Alloy 600 is an example, which is used in the nuclear industry in heat exchangers, and it is vulnerable to a form of cracking called stress corrosion cracking (SCC), and that is a highly challenging material failure type. The presence of films consisting of Cr- and Fe-rich oxides along grain boundaries directly cause SCC failures [59].

During the particle impact in a cold spray, the brittle oxide skin, which covers metal surfaces, shatters that sweeps away when a high-velocity gas jet is used, which uses particles to prepare a surface. As compared to the original powder, the cold spray deposits have equal or lower oxygen [65]. Figure 3.3 shows the thermal properties, porosity, and oxygen content of Al, C, and Sn, when they are sprayed using cold versus thermal spray. A cold spray diminishes oxygen content in the deposit, which is useful for future applications. For instance, the intermetallic compounds' deposition of FeAl-based intermetallic alloys shows promising excellent corrosion resistance and mechanical properties for sulfidizing and oxidizing atmospheres at a high temperature.

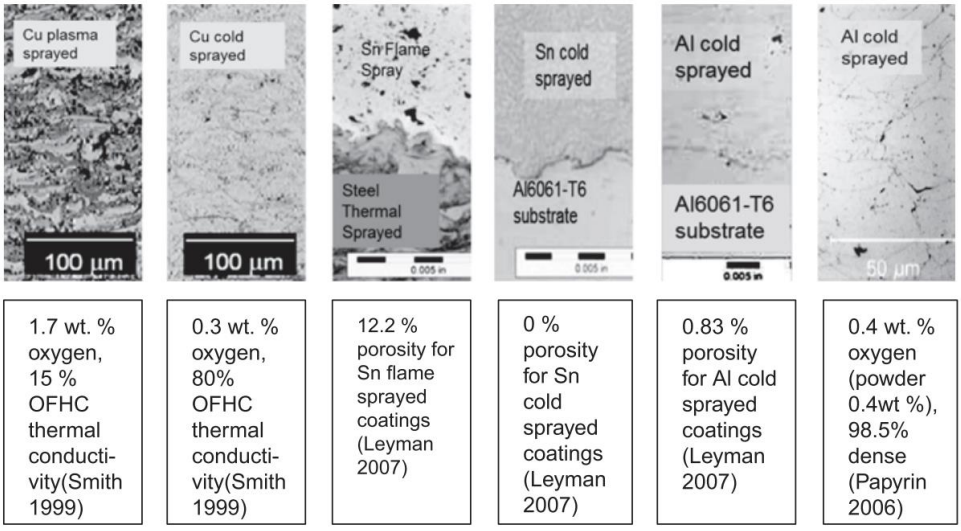

Figure 3.3. Thermal spray versus cold spray based on oxygen content, porosity, and thermal properties [59].

The mentioned substances are lighter (5.56g/cm3) as compared to Ni-based alloys or steels because they have high creep strength and melting point in addition to impressive thermal conductivity and low cost. They can substitute Ni-based super alloys or even stainless steels because of the mentioned attributes for performance at a high-temperature [70]. The intermetallic Fe–Al have low ductility at a low temperature. It happens because their mechanical strength reduces at more than 600°C. Different thermal sprays, including HVOF, plasma, flame or wire arc spray are used when FeAl-based alloys need a spray to protect carbon steels against corrosion but the mentioned deposits result in the formation of oxide content that provides limited

corrosion protection. It happens because of a significant melting point difference between Fe and Al and the exothermic nature of iron aluminides [70,71].

Cold sprays can be used to spray Fe-Al-based materials using powder blends, after which, an annealing post-spray is performed [72], which completely transforms a Fe(Al) solid into an FeAl inter-metallic [70]. Powdered mixtures, including Al/Ti, Zn/Al, Al/Ni, Ni/Al, Ti/Al, and W/Cu are cold sprayed. Later, they are annealed and a dense well-dispersed intermetallic distribution is obtained [70,72].

3.3.6. High Density, Low Porosity

A thermal spray deposit has an outer zone, which has a typical lamellar structure, and it shows splats, which are loosely bonded together, and they create many micro-sized pores [73]. High porosity level (5–15%) has been observed for arc and flame spray but for a plasma spray, it is 3–8% that means it is corrosive [74].

Cold spraying has no splashing, and it is a solid-state procedure. It is performed at a high speed, which is above a material's critical velocity, and the particle impact on the substrate at a high strain rate. They plastically deform and it results in bonding. Additional thermal energy is generated at interfaces when high-strain deformation takes place that generates interfacial metal vapor jet, which further produces a material's "vapor deposition" that fills the existing cracks and pores. This way, cold spray combines microscopic and particulate vapor deposition procedures [61]. Moreover, the spray plum's each subsequent pass performs "shot peening" on the layers below, which increases their overall density. It combines with a cold spray, which results in excellent and dense coating [61]. Additionally, when we apply post-spray heat treatments, the deposits further consolidate and densification occurs at ideal levels because of closure of inter-splat boundaries, cracks, and pores (Figure 3.4) [75].

3.3.7. High Thermal and Electrical Conductivity

Coating quality indicates electric conductivity while other indicators include presence of dispersed oxide phases and material density [76]. Since copper has exceptional

thermal and electric conductivities and it is commercially available, it is a significant substance in today's industries [57]. We know that if an oxide is present in a plasma-sprayed copper coating, it reduces the deposits' electric conductivity by almost 15% as compared to the oxygen-free high-conductivity (OFHC) copper [67]. Contrary to that, a dense copper coating displays conductivities above 85% of the OFHC copper [65,67]. Similarly, a copper material typically displays almost 40–63% conductivities as compared to OFHC copper if they are sprayed using a conventional thermal spray. After a cold spray, post-annealing increases the deposits' conductivity by recrystallization and densification but it is performed only in case a manufacturer can afford it [57,76].

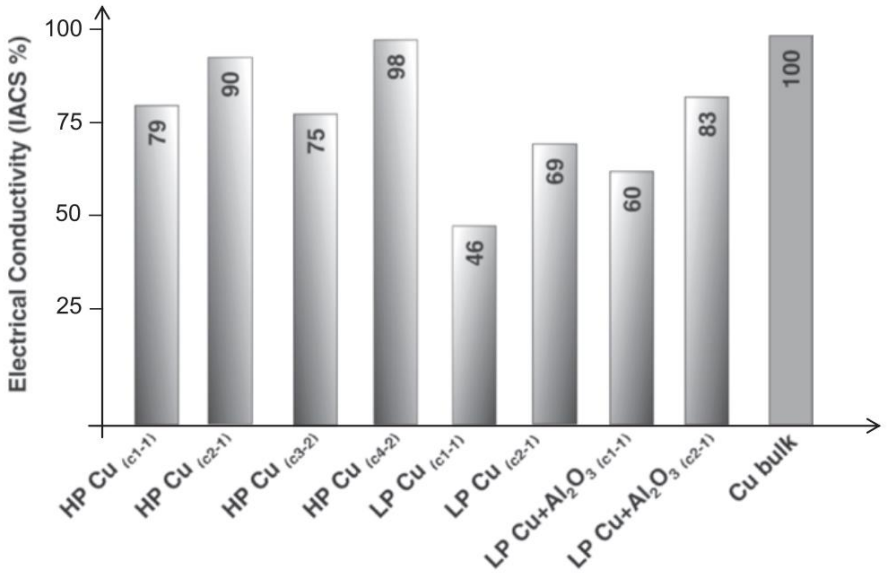

Figure 3.4. Electric conductivities of copper coatings through cold spray. Here, LP represents a low gas pressure, HP stands for high gas pressure, and IACS stands for International Annealed Copper Standard [59].

In Figure 3.4, electric conductivity of sprayed copper coatings has been compared, which used downstream and upstream injections (LP and HP), and they conduct the overall cold spray procedure. The average of values is given by the IACS values, and they are measured by applying a measurement process consisting of four points considering the steel surfaces: (c1) sprayed steel, (c2) heat treated steel at 400°C, (c3) ceramics, which are heat treated at 280°C, and (c4) heat treated ceramics at 280°C. Authors Koivuluoto [76] and Donner [77] have sufficiently explained the given

phenomena. Copper coatings are produced with an upstream process at HP that uses high electrical conductivity for producing copper coating as compared to the downstream injections working at LP but when a downstream injection is combined with powdered blends (Cu+ Al_2O_3) and used, electrical conductivities are attained when the deposits are sufficiently densified, and the conductivities are sufficient for a majority of electric applications. Al_2O_3 particle additions perform a main function to activate (roughening/cleaning) the lower surfaces and hammer-deposited particles to build up a high-density and low-oxygen deposit, which is highly receptive to sprayed particles' fresh impact and adhesion.

3.3.8. Bond Strength

A deposit's cohesive and adhesive strengths are significant to assess its usefulness for a specific application [78]. Generally, both strengths can be determined when a spray is done on the cylindrical tensile sample's top surface before it is glued to a counter-body. Then, certain materials are combined and the assembly faces tension to failure (ASTM-C633). Using some material combinations, this method is used, and it is clear that the deposits may cohesively fail by forming a fracture [79] or it can adhesively fail when the fracture formation is at the substrate or deposit interface [80]. The addition of ceramic particles (Al2O3) and pure aluminum substantially increases cohesive or adhesive strengths [80], [81]. The test results are limited because of the glue strength. In order to deal with this limitation, some researchers [78] tried other testing processes, which indicate that cold-sprayed deposits result in superior adhesive strengths (almost 250MPa in case of aluminum alloys) [65].

3.3.9. Compressive Residual Stresses

Generally, the surface tensile stresses contribute towards forming and propagating micro cracks that increase fatigue failure. Since thermal contraction or expansion takes place while solidification or melting, the thermal spray deposits create residual tensile stresses [74].

The cold spray procedure has a distinct feature, which is its superficial compressive residual stress development [82]. Compressive stresses have exactly the opposite effect on fatigue life.

It is shown through modeling and experimentation that cold sprays generate the needed compressive stresses on the surface. They improve certain materials' fatigue life. Applying low-pressure downstream injection, Al7075 is cold-sprayed over Al5052 substrates, which showed almost 30% improvement in fatigue life [83]. Some researchers have reported almost 10% fatigue life improvement when aluminum was cold-sprayed over AZ31B magnesium substrates [59]. During the cold spray process, compressive residual stresses are generated, which contribute to the formation of ultra-thick and well-bonded coating for achieving net-shaped components, which are made up of composite, polymeric, and metallic materials [74].

3.3.10. Corrosion Resistant

Traditional thermal sprays, including air plasma spray, twin-wire arc spray, and flame spray have some common aluminum deposit methods, through which, aluminum is deposited on steels and other substances to protect against corrosiveness. Despite the fact that they are generally less expensive in comparison with the cold-spray, intense phase transformations, high porosity, and oxidation become conducive for comparatively poor corrosion performance in comparison with dense materials [73,75]. There are some environmental challenges linked to the mentioned processes [84]. Phase purity, homogeneous microstructure and high density are some benefits of cold-spray.

Coatings sometimes result in exceptional corrosion resistance [65]. Now, cold sprays are becoming a preferred choice for localized corrosion protection and repair for several applications, and for some applications, no other option is feasible or available [84]. Some applications, including automotive magnesium castings and aircraft bodies require this process [84,85]. Other researchers [64] have experimentally mixed it with stainless steel (316L) particles using Co–Cr alloy (L605) particles, and the latter exhibits higher corrosion resistance as compared to the aforementioned 316L category

but that is difficult-to-manufacture. Studies show that cold sprays are helpful to consolidate metals when they are applied as a blend (33% L605 and 67% 316L), which is later heat-treated to improve the corrosion resistance as well as mechanical properties to make the composite better than 316L, which are now in the process of becoming a whole new metallic biomaterial category [64].

3.3.11. No Masking

Traditional thermal sprays require masking hot particles through over-spray, which stick to outside-the-target surfaces, and commonly, masking is manually accomplished that adds to the overall manufacturing cost [67]. For instance, the repair and assembling blade specifications in power turbines need a sealed layer of abradable aluminum, which is applied to each blade's base that connects to the main shaft, which reduces leakages that might otherwise significantly reduce the efficiency. Traditional thermal sprays need excessive masking that stops the remaining part of a blade from overspray but it results in significant price increase [59]. Heat conductors and electric circuits of many industrial applications require patterned deposits; therefore, cold sprays are ideal because without needing a masking procedure, they can spray in well-defined patterns. Using a nozzle exit diameter, the track width is controlled and the new applications need narrower tracks as compared to the standard nozzle diameters [86]. Practically, nozzle modification is done so as to squeeze the cross section, which is significantly smaller (1–2mm) as compared to the longitude [65]. The change in geometry has no significant effect on particle velocity [87]. For additive manufacturing, there is a possibility of using cold sprays and smaller nozzles should be developed, which are capable of delivering small footprints to improve the shape.

3.3.12. Flexibility in Substrate–Coating Selection

For selecting coating–substrate combinations, cold sprays have been used. Previous researches show different types of coatings: Al–20Sn and Al–10Sn substrates on Al6061, US304, and Cu [88], Al on Ni substrate [89], Mg powder on aluminum plates and stainless steel [85], Al-5Fe-V-Si aluminum alloy on an internal combustion (IC) piston heads [90], Cu + Al_2O_3 on steel substrate [91], bi-metallic Al/Cu and Al on

reinforced carbon polymer matrix composite [59], and Ti + SiC and Al + SiC mixtures on steel as well as aluminum surfaces [92]. Cold spray bonds combine metallurgical bonding and mechanical interlock while the nature of the substrate is less significant; so, several incredible combinations are possible.

3.3.13. Coupling Dissimilar Materials

It is possible to couple dissimilar substances to make exotic products with impressive properties to explore some new fabrication processes. For instance, the aluminum alloy substrates' wear resistance is possible to be enhanced using cladding on alloys of iron but in traditional cladding processes, the required heat input may result in undesirable intermetallic phases, for example, Fe_3Al, FeAl, Fe_2Al_5, and Fe_2Al at the interface, which induce crack failure when a sample is cooled down [93]. Other cases show that steel substrates require corrosion protection, and for that purpose, an aluminum layer is typically deposited with the help of a twin-wire arc spray.

It is a fact that the latter is common and the resulting porosity helps forming interconnected paths in a coating, which permits corrosive electrolytes to access the steel substrate [94]. This kind of corrosive behavior can be observed in different coatings, which are done through HVOF, plasma spray, and flame spray [94]. Since it has a low process temperature that combines with high particle velocity, and dense deposits of many materials, it can be accomplished through the cold spray procedure. Such materials include copper, aluminum, 316L, Ti64, and nickel, which are coated on dissimilar substrates [59].

Metals like copper and aluminum can be directly cold sprayed on some polymeric surfaces and unprepared and smooth glass surfaces [59]. Contrary to that, polymeric substances (like polyethylene) can also be sprayed on an Al 7075 substrate. Mixing diverse materials makes a cold spray good for free forms, which have customized properties and different engineered metal matrix composites (MMCs) [95].

3.3.14. Ultra-Thick Coatings

When conventional thermal sprays are used for building thick deposits, it is progressively buildup through superficial tensile stresses because in this case, thickness increases but there is a progressive decline in the bond strength. Ultimately, the material's resistance overcomes the stress buildup, which causes spontaneous delamination or spalling. Cold spray coatings, unlike other thermal processes, are compressively stressed on the surface; so, eliminating or minimizing it through thickness gradient, which is created when thick coatings are produced using a thermal spray, is essential [65].

3.3.15. High Deposition Efficiency

It represents a ratio that is generally expressed in the form of a weight percentage of the powder, which is deposited on a substrate, to the weight of the sprayed powder [59]. Higher deposition efficiency (DE) is not compulsorily linked with improved spray-ability because certain substances are readily deposited; however, the case is the opposite when the deposit has poor properties, including poor bond strength or high porosity. DE is not just linked with the particle's surface condition and nature but the impact velocity or amount of kinetic energy as well. Generally, higher DE values (above 95%) are possible because of high-impact velocities specifically when aluminum or copper are deposited. When helium is used, it is possible to attain very high impact velocities at high temperatures and pressures but that is a pricy option. Contrary to that, it is possible to attain high DE values at lower impact velocities through the spray powders' characteristic manipulation. DE is a significant material cost consideration but that depends on the kind of materials, which are sprayed. Mostly, it is significant for health and safety because waste metal powder collection and disposal have a significant cost.

3.3.16. Environmental, Health and Safety

For chromium plating, hexavalent chromium is used, which is an officially declared human carcinogen but now, their users are switching over to tungsten carbide HVOF

thermal sprays [96], which is a safer option. Since combustible gases, flames, fumes, and sparks do not exist in the cold spray, it is a great alternative spray process with respect to health and safety [63]. In cold sprays, electrolytic hard chrome (EHC) plating is replaced by WC–Co coating [59]. Other highly-operational risky scenarios require a portable downstream injection cold spray, which is effective for remote corrosion repairs when aluminum vessels containing heavy water for nuclear reactors need repairs [59]. To cast iron canisters, thick copper coatings are created using the cold spray technology, which is now considered as a reliable process, and it is helpful to dispose-off nuclear wastes [59].

The surface applications of medical antibacterial substances is another case, which has become interesting for the researchers. Copper has well-documented antibacterial benefits and depositing dense copper through cold spray on many surfaces is one of the important applications. According to some researchers, using inoculants through a spray can make it three times more efficient for bacterial elimination as compared to conventional procedures. Meticillin-resistant Staphylococcus aureus (MRSA) makes cold sprays an excellent option for food processing, air-conditioning and health care applications [97] but cold spray is not without issues. The cold spray technology results in several health, environmental, and safety risks, which are linked with waste powder management and the process noise.

3.4. COLD SPRAY LIMITATIONS

Like other processing techniques, cold spray has specific limitations, which depends on its evaluation perspective, which is given below:

3.4.1. Almost Zero Ductility

The main disadvantage of cold sprays is their essential plastic particle deformation that decreases the coating ductility. A research [12] showed that after a cold-spray, aluminum coatings show elastic modulus on a pure aluminum plate (A1050), which is more than the aluminum substrate's corresponding elastic modulus that shows early cracking signs during tensile loading. No cracking has been observed on the cold-

sprayed aluminum, when compressive loading was applied, which resulted in more strength than a cold-rolled aluminum. After annealing, a cold-sprayed specimen readily restores ductility at less than 270°C as compared to untreated samples, which is quite interesting. The stored energy is great because plastic deformation takes place in cold-sprayed materials because they recrystallize and consolidate when a material is heated.

3.4.2. Limited Range of Sprayable Materials

Many thermal sprays deposit different materials ranging from metals to ceramics whereas a cold spray just deposits composites or metals to a satisfactory level to assure ductility at a low-temperature, for example, some metals like Cu, Ti, Al, Zn, Ni, Ni, Ag [98] and their blends with other non-ductile species or ceramics, such as WC–12Co blended with Ni, Al–Al2O3 mixtures, Al–12Si alloy composites, and WC–Co blended with Cu or Al [80]. For many years, researchers have been trying to increase the types of materials, which can be cold sprayed. Some exotic efforts have been conducted on SiC (no metal matrix binder) on Ni–Cr-based super alloys and Al–Ni intermetallic compounds to increase high-temperature oxidation resistance [59] but most of them are impossible to deposit with the help of other thermal procedures.

3.4.3. Substrate Material should be Hard

A hard substrate material induces satisfactory incoming particles' plastic deformation for a good bonding level [65]. On one hand, very soft substrates (like polyethylene) cater the incoming particles beyond the surface without any buildup possibility while on the other hand, brittle substrates, which easily delaminate (carbon), undergo erosion because of the incoming particles. To accept a coating, substrates should be well-supported or resilient.

3.4.4. Gas Consumption

In a cold spray procedure, gas consumption is more than several other thermal spray procedures because it offers high velocity and increased flows, which propel the

particles. Nitrogen, helium and air are the carrier gas choices, and their use depends on the need for density. Helium is highly desirable because it can assure high gas velocity and inertness. Helium produces better quality but it is expensive and scarce; therefore, its use is limited to specialized applications only, and recycling of helium becomes essential that increases the overall complexity of cold sprays [98]. Thus, during the last few years, experts are trying to develop cold spray methodologies to operate using air or nitrogen with/without air for all cold spray equipment and sprayable substances. The cold spray's upper operational range with nitrogen can be as high as 1000°C at 70 bar pressure. Operational parameters, which are needed for spraying materials include low-temperature ductility, which should be lower than the conventional cold sprayable metals, for example, titanium alloys, Ni-based super alloys, tantalum and stainless steel. In the mentioned operations, gas consumption and operational and capital costs are very high; therefore, their application should justify the costs. The actual operational and technical needs of the intended applications form the basis for a decision on a specific cold spray system.

3.4.5. Line of Sight

Cold spray has similarities with other thermal spray procedures; however it is quite unlike some procedures, including physical and chemical vapor deposition and electroplating, so, it is a "line-of-sight" procedure [99], and this is why, it is hard to spray the inner surfaces through this process, for example, internal pipe surfaces without changing the nozzle design. In cold spraying, the standoff distance should be 10mm, which is unlike traditional thermal sprays because it is significantly shorter. Thus, designing nozzle assemblies to fit in the cavities is easier because otherwise, spray tasks would have been impossible. Until now, commercial cold spray equipment manufacturers have supplied 90° nozzle assemblies, which can spray the pipes with even 90mm diameter.

3.4.6. Limited Availability of Standard Specifications

Until now, just a single standard specification (MIL-STD-3021) has been brought to the public domain from the military research labs but several companies already own

cold spray equipment using their specific internal sprays, and some of them have developed their own specifications. Some early adopters are operating transportation and aerospace companies.

3.5. PHYSICS OF COLD SPRAY

CS or cold spray is one of the several thermal spray procedures. It deposits materials in the form of micron-size solid particles, which accelerate to higher speeds before affecting the substrate and it produces a coating by bonding mechanisms and complex deformation. Producing almost net-shaped parts is possible as an additional manufacturing processes. CS has a growing interest, which is linked with continuous search to find the optimum spray conditions to decrease the process cost and increase the coating properties. CS is considered as a fully established process for metal repair/coating production that is effective for additive/net-shaped rapid processing. After two research and development decades, different commercially viable CS systems are now commercially available. Through a pressurized propellant gas flow, particles accelerate at a high-impact velocity, which expand through converging–diverging moves and de Laval type nozzle is used in such cases [100].

Powdered particles predominantly accelerate in CS using a supersonic gas jet portion (diverging section) that has a lower temperature as compared to the melting point of a material, which forms a coating that remains solid during the flight. Consequently, processes like thermal residual stresses for conventional thermal spray, evaporation, crystallization, melting, and high-temperature oxidation have harmful effects, which are eliminated or minimized. Deleterious effects of melting at a high temperature on substrates and coatings offer significant advantages and certain new prospects, which make the CS viable for different industrial processes.

It is already understood that in CS, material deposition takes place through subsequent deformation of particles and high-velocity impact [98]. For bonding, the most significant factor is the particle velocity. If the particle velocity (Vp) exceeds the critical value (Vc) after bonding [101], the critical value is the minimum velocity, which a sprayed particle should have depending on the substrate type. Generally, for

packing density and optimal deposition efficiency, it is essential to assure high-particle-impact velocity. Coating quality and deposition rate directly depend on several parameters. Moreover, several parameters are interlinked, which makes investigating their independent impact a difficult job. Despite the fact that all the CS parameters have impact on the coating quality and deposition rate while some of them are more significant. There are four categories of major parameters:

- Spray setup: It involves material traverse speed, nozzle geometry, standoff distance (distance from the substrate), and orientation [100].
- Substrate: It includes the surface temperature, nature of the coating material and its surface preparation before spraying.
- Feedstock material: It includes selected powder characteristics, like their particle size, material composition and particle geometry, distribution of size, particle feeding rate and practical impact temperature.
- Propellant gas: The gas stagnation pressure, temperature and nature.

3.5.1. Process Parameters

Fig. 3.5 shown the schematic diagram of a typical CS system. For generating a driving flow, which accelerates powder particles, high-pressure gas supply (air, helium, nitrogen) is needed. An electric gas heater heats this flow, which allows operations at high gas temperatures, which range from room temperature to 1200°C.

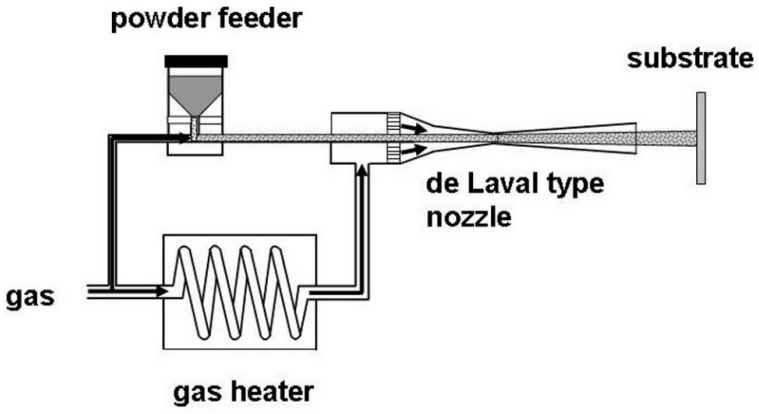

Figure 3.5. Schematic of the cold spray technique [102].

The gas is primarily heated to achieve higher gas velocity, which results in greater particle velocities. The feedstock particles get soft, which takes place during the CS, and it is helpful in a few cases. A converging/diverging nozzle (de Laval) is fed on the driving flow, and through converting the thermal energy into kinetic energy. Then, it accelerates and expands at a supersonic speed [99,102]. The velocity of gas is a function of the gas condition (temperature and pressure), gas type and nozzle geometry. The powder feeder is fed through a feeding flow and the powdered particles enter a nozzle. Over there, they accelerate through a propellant flow. The impact velocities' range is 300-1200m/s that depends on the spray parameters and the process gas. Various factors are responsible for the particle impact temperature, including nozzle design, gas temperature, and nozzle and particles' heat capacities. Sufficient kinetic energy is needed for particles to drive the gas impact on the substrate, deform plastically and coat on the surface. The particles, which do not affect the substrate surface, possess enough kinetic energy, which makes it possible for the particles to plastically deform and form a bond in the shape of a coating. The particles, which have insufficient velocity, bounce off and they can erode the surface [58].

3.5.2. Nature of Propellant Gas

As mentioned earlier that during the CS process, a gas accelerates the powdered particles at a high pressure, and the powdered particles are moved through a secondary flow towards the nozzle. Practically, any pressurized gas is suitable for this purpose but air, helium (He), or nitrogen (N2) should be used. Nitrogen and helium are inert, which is an advantage. Obviously, gases, which have lower molecular weights, like helium, are useful because their velocities are higher in case of specific nozzle geometry. According to pure thermodynamics, helium is the best option but its cost is a major issue, which makes it economically unviable because additional cost is paid when helium is either recovered or recycled; therefore, a helium-nitrogen mixture is used as the driving gas in some applications. Since nitrogen is diatomic and when it is added to helium, the overall enthalpy of a carrier gas rises, which improves heat transfer but that happens because of gas velocity and the atomic mass of the gas mixture, which results in softer and less denser coatings [103].

3.5.3. CS Bonding

When a metal fractures, both surfaces come in contact with each other, and this process takes place in a vacuum, it forms a cohesive bond, through which, the strength becomes equal to the strength of a parent metal [100] but to assure a strong bond between the metal powder particles, the metal surfaces, which are exposed to air, need to be covered using organic contaminants and a native oxide film. To form strong metallurgical bonds between the metals, metal lattices should be in the intimate contact while the layers are removed.

Particles strike an already deposited layer or the substrate at a very high velocity in CS, which deforms at an extreme strain rate at the interface (up to 109s−1) [14,104]. At the contact surface between the receiving surface for strong bonding and the impacting particles, this creates necessary conditions for strong bonding to happen. It is not trivial to establish exactly what these conditions are. In this context, we must counter the following difficulties:

- Very small but demanding high-resolution length scale is needed for bonding to occur. Generally, amorphous and intermetallic layers and oxide films are just a few nanometers in thickness.
- Since CS is used to deposit on various materials, assuring consistency of particle morphology and material purity from a powder batch is not possible while real powders have different particle size distributions, and those particles have a broad range of angles and velocities when they leave the CS nozzle.

The particle geometry flattens and generates a broad spectrum of deformation states for each particle. Consequently, at any point of the interface, physical conditions may be unknown in the same way as they are in the processes that involve the molecule-by-molecule or atom-by-atom material deposition [100].

3.5.4. Critical Velocity

Papyrin et al. discovered CS in Russia during the 1980s when it was recognized that solid particle deposition just happens for a limited range of particle velocities and sizes. At low velocities (order 101–102m/s), bodies get exposure to repeated particle impact, and they undergo erosion. At less than 100m/s particle size, submicron-sized particles impinge and stick to the surface but it is not linked to the CS, which involves strong bonding and material build-up in layers among the particles [105]. Critical velocity (Vc) is the most significant physical limit to overcome.

Material loss takes place through substrate erosion below Vc. When particles deposit, material gain is assured above Vc. Sufficient particle acceleration can be produced that exceeds Vc when a high-pressure gas is used, the gas is preheated, and the nozzle has a particular design.

When the velocity is too high (more than 3000m/s), we entered a field of hypervelocity, in which, the impact greatly stresses and the stress exceeds the material strength, which results in strong shock waves. At this stage, solid materials act like liquids [106]. Transition takes place from deposition to strong erosion during a high-velocity CS. A study shows that the mentioned transition takes place at about 2Vc [107]. The strong erosion threshold is unattainable for several materials with high Vc, but this does not happen when helium is applied. The focus is actually maximizing particle acceleration to enable most particles to exceed Vc.

3.5.5. Transition from Erosion to Deposition: Deposition Efficiency Curves

Some sprayed material either rebounds or splashes away in several thermal spray processes, and they are not ‘captured’ in the coating, which results in lower than 100% process efficiency. According to Eq. 3.1, the term deposition efficiency (DE) can be mathematically expressed as given below:

$$DE = \frac{\Delta m}{M_0} \tag{3.1}$$

Here, Δm represent the increase in the sample weight during a spray while M_0 shows the total material mass, which is thrown at the sample.

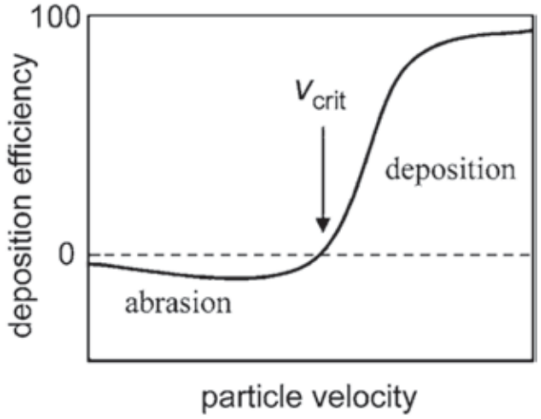

Figure 3.6. Idealized deposition efficiency curve [109].

The identical DE definition is used at a low-temperature with solid-state particle impingement. A vast majority of particles elastically rebound at low velocities (less than 200m/s), such as the one, which is encountered during a peening or micro-grit blasting operation. Just a few of them are embedded or they loosely stick; therefore, DE will be almost zero or close to it. The loss of net mass happens because of substrate erosion.

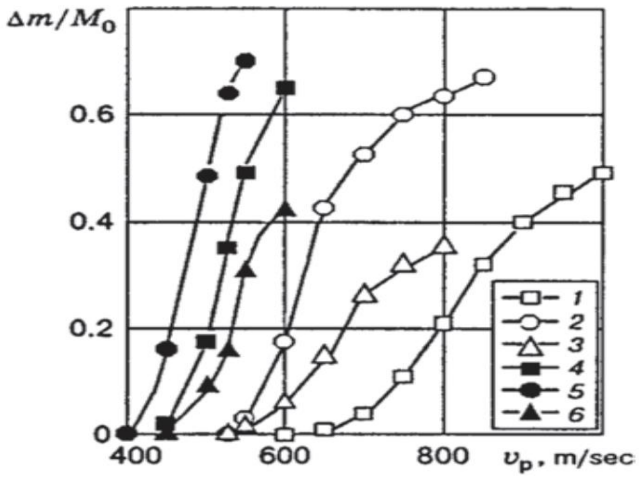

Figure 3.7. Particle velocity versus deposition efficiency [110].

1-aluminum, 2-copper and 3-nickel. (Helium-air mixture is used to accelerate it at room temperature.) 4-aluminum, 5-copper and 6-nickel, for which, hot air is used.

In case, the sprayed particles show a certain ductility level while the spray system accelerates the particle velocity. DE begins a steep rise. DE can eventually lead to 100% with sufficiently high impact velocity, which depends on the material of the powder. An idealized response to DE increases particle velocity, which is shown in Figure 3.6. The CS process has some early DE measurements, which use different metal powders, as given in Figure 3.7 [100].

3.5.6. Effects of Material Properties on Critical Velocity

For various applications, the coating industry has attempted to spray new materials. CS was only used for copper, aluminum and nickel during the early development stage but it is now a fully functional industry, so now, CS is successfully applied to deposit several alloys, metals and metal–matrix composites. A low mechanical strength (low deformation resistance) and a low melting point are common material attributes, which are hopes for CS to become a functional coating procedure. They include pure copper, aluminum, silver, zinc, tin and alloys. All the mentioned metals have low yield strengths. At elevated temperatures, they show significant softening. Large number of studies are now available, which discuss depositing Cu and its alloys [108] and Al and its alloys [109]–[111]. It is shown in Fig. 3.8 that copper, nickel, and aluminum powders have less-than-50µm particle size and their V_c ranges between 500–600m/s. According to Assadi et al., the V_c is 660m/s for less than 45µm aluminum and 570m/s for 5–22µm for copper [14]. They are metals of the iso-mechanical group, which were classified by Ashby and Frost [100]. A face-centered cubic (FCC) crystal structure is common among them and their bonding is also similar. FCC lattice might cause a slip that happens along the closely-packed plane; so, FCC metals are deformable.

Contrary to that, a few less deformable hexagonal closely-packed (HCP) metal sliding planes are available. Titanium is also useful because it has 750m/s V_c [112]. Different studies throw light on Ti, its alloys, and their deposition [113,114]. There are no closely-packed planes in a body-centered cubic (BCC) lattice. Their coordination number is less than FCC or HCP; so their deformability is the poorest [115]. Other than the major crystal groups, alloying normally reduces deformability. Consequently, alloys have more Vc as compared to pure metals. Nitrides, oxides, many ceramics and

many carbides are brittle; so cold spray cannot be used on them. Thin ZrO_2 layers [115] or TiO_2 layers [116] were reportedly deposited onto metallic substrates using conventional CS equipment; however the substrate deformation is needed. Coating build-up ceases once the substrate is covered. According to Xu and Hutchings, polyolefin can be deposited using CS at DE < 0.5% and 135m/s velocity [117].

Powder blend CS has just a single metallic component while the other one is an alloy. A ceramic or inter-metallic is applied, and it is quoted with a metal–matrix composite (MMC). Through deformation of plastic metallic components, dense deposit build-up and bonding take place, and the hard component is prevented from rebounding through metal particle deformation. According to the literature, MMC compositions between 10:1 and 1:1wt.% were successfully deposited [30,80,92,118]. When a pure metal is sprayed, hard particles are included, which results in peening that densifies and compacts a coating that boosts the strength between the coating and the substrate [119, 120].

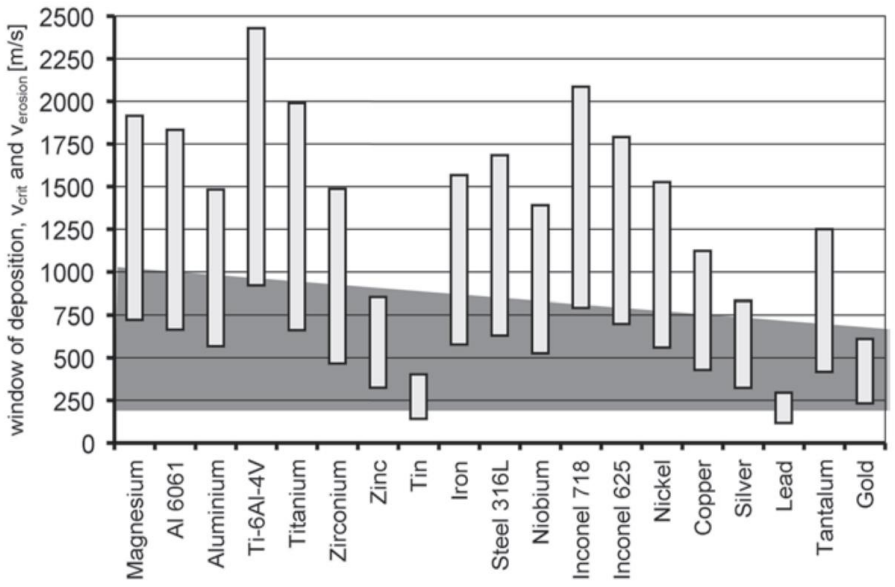

Figure 3.8. Critical velocities and deposition windows at 20°C impact temperature for different substances [102].

Deformability is a prime consideration for CS metal and alloy bonding. Some factors, which specifically influence V_c, include density (ρ) and melting point (T_m). Figure 3.8 shows that aluminum deposit is more difficult as compared to Cu or Ni despite the fact

that the three metals belong to the same iso-mechanical group. The low aluminum density (2.70g/cm³) decreases the energy impact in comparison with copper (8.96g/cm^3) or nickel (8.91g/cm^3). Moreover, it has high specific heat capacity (C_p) that makes it difficult to assure the required shear instability.

This analysis effectively ranks the different material properties' relative influence and it lets V_c plotting to go out of range for metals/alloys, which is certainly practical [107], [121]. First, we empirically measured the critical velocities for limited types of particles based their sizes, temperatures, material properties, and extended their results to other substances (Figure 3.11). The top of each bar shows the upper erosion limit for each substance in Figure 3.11. It is determined using mass loss measurements, which have single millimeter-sized spheres. They have been extrapolated in the size range of CS. Despite the fact that spray trials of most materials have been reported in Figure 3.11, systematic comparison among V_c values of several substances is lacking. It is surprising to see the contrast between the high-V_c titanium and nickel alloys and low-V_c materials, like lead, tin, and gold, which shows that CS applications are needed to improve the conditions for CS.

3.5.7. Effects of Purity and Particle Size

It is important to note that for developing new CS applications, some researchers chose coarse and traditional spray powders. There are different bonding and deformation mechanisms in CS as compared to thermal sprays, which require a serious investigation by industrial powder developers, producers, and researchers in order to make better feedstock powders for CS. Schmidt et al. [107,112] have presented an excellent discussion on particle size and its impact on V_c. There are many factors, which show that the critical velocity reduces when particle size decreases. Since surface area-to-volume ratio of small particles is higher, they have higher impurity levels, for example oxygen. When powders are produced after cooling a melted substance (atomization), it results in higher quench rates for small particles. Smaller grain size is the consequence, which further results in Hall–Petch hardening. The CS process results in strain-rate hardening for particles, which have small dimensions.

Because of steep thermal gradients, thermal diffusion has a limited impact on peak interfacial temperature.

Larger particles show more inertia, which makes it hard to accelerate; so, an optimum particle size range exists that does not have very small particles to let the mentioned effects dominate but they are not large enough to increase the energy demands. This range can be 10–45µm for ductile materials like copper [107]. Material purity is another significant consideration for a CS powder. It is obvious from artificial oxidation of copper, aluminum [122], Monel powders, and 316L stainless steel [123], in which, increased oxygen raises V_c. On metal powders, oxidation has a twofold effect. First, it loses ductility because of interstitial hardening, oxide dispersion, and decreasing deformation. Second, it changes the thickness/structure of an oxide film surface that impedes bonding [122,123]. When V_c values are compared, we must consider the effects of purity and particle size distribution. Moreover, lack of a standardized measurement process results in some variations, which have been reported by different researchers. Seven values have been reported for copper's critical velocity in Table 3.1.

Only Li et al. reported an exceptional measurement of 327m/s [124]; otherwise, the values ranged from 520 to 610m/s. First, 327m/s appears odd but Li et al. used smaller particle sizes and purer copper; therefore, their oxidation tests are considerable; however, a realistic oxygen concentration specification is 0.1–0.2wt.% for less than 25µm powder for industrial applications. Other important factors include crystal structure, material purity, temperature at impact, and alloying, which make it clear that cold-sprayed particles' bonding is linked with their deformation. To understand this relationship, physical processes should be considered in more details, which occur when CS particles flatten and deform.

Table 3.1. Critical velocities of copper.

Reference	Particle size (μm)	Powder properties	Measurement technique	Critical velocity (m/s)
Assadi et al. (2003)	5–22	Inert gas atomized, 99.8% purity	Deposition efficiency, combined with particle velocity distribution by CFD, verified by laser Doppler anemometry	570
Gartner et al. (2006)	5–25	Spherical morphology, oxygen content <0.2%	Deposition efficiency, particle velocity determined by CFD	550
Raletz et al. (2006)	10–33	–	Deposition efficiency, particle imaging	538
			Particle imaging, velocity calculated by 1-D isentropic model	520
Li et al. (2006)	Average 56	Gas atomized, oxygen content ~0.01%	Deposition efficiency, particle velocity determined by CFD	327
		As above, oxidized to 0.14% oxygen		550
		As above, oxidized to 0.38% oxygen		610

CFD computational fluid dynamics

3.6. WEAR PERFORMANCE

One of the latest emerging technology is surface modification, which has the potential to effectively change/improve the main surface properties. Material deposition with higher wear and corrosion resistances is possible using different methods. Both chemical and plasma vapor deposition generate protective layers of ceramics like ZrCN, TiCN, Al_2O_3, and TiO_2 on a substrate [125]. Other process costs of deposited layers are not so high, which helps maintaining the coating-substrate bonding at a high level. Moreover, both plasma and chemical vapor depositions have limitations in terms of applicability to complex components with shadowed or dead corners. Plasma electrolytic oxidation and anodizing [126] are approaches used for obtaining hard oxide and corrosion-resistant layers. These layers can provide wear and corrosion resistance but they have small thickness and such layers are formed with pores that initiate sites to deposit corrosion. Often thermal spray coatings are significantly porous that reduces corrosion resistance of coatings on active substrates. When no post-

coating procedure is performed, like hot pressing or epoxy sealing, the coating is often inappropriate for active substrates as protective coatings [127–129].

If we consider the commonly applied surface modification methods and compare them with the cold spray technique, the cold spray provides a comparatively better surface protection, and now, it has become an emerging process to generate economical bulk coatings with net-shaped material deposition [130,131], which makes it an attractive option because it can deposit combinations of metallic and non-metallic powders at a lower temperature than the melting points of the substrate or the coating. During the deposition through cold spray, the powdered particles go through a stream of gas, which is accelerated at the speeds within the range 500–1000m/s, depending on the gas consumed, size and density of the powder particles. In this process, the gas is heated, which increases the coating speed, it softens the particles and enhances the effects of their deformation on bonding as well as its impact [125].

PART 4

MATERIALS AND METHODS

4.1. EXPERIMENTAL PROCEDURES

4.1.1. Coating Material

The EN 10130 steel substrate material was used. Before cladding, the surface of the block samples was prepared by grinding with 1200 grit SiC paper and ultrasonic cleaning with ethanol. The matrix material in the powder combinations consisted of spherical Al (99.6%), Ni (99%), Zn (96%), and Sn (99%) powders with a mean particle size of 15µm. Al_2O_3 powder (99.4%) with a mean particle size of 20µm was employed as reinforcement. OCPS Ltd provided all of the powders. The powder composition and ratios are listed in Table 1.

Table 4.1. The powder composition used in the study.

Samples	CAS#	Chemical Name	Wt, %
A1	1344-28-1	Aluminum Oxide	60-70
	7429-90-5	Aluminum	40-30
A2	1344-28-1	Aluminum Oxide	45-50
	7440-66-6	Zinc	50-55
A3	1344-28-1	Aluminum Oxide	41-45
	7440-02-0	Nickel	55-59
A4	1344-28-1	Aluminum Oxide	45-55
	7440-31-05	Tin	55-45

4.1.2. LPCS Procedures

A Dymet 423 gun with a Laval nozzle was used to create a low-pressure cold spray (LPCS) coating. The nozzle's throat diameters are 2.5mm and the exit diameters are 5mm. The gap between gun passes was adjusted at 2mm. The driving and carrier gases were both air, with a stagnation pressure of 620 kPa. The temperature of the gas just before it entered the nozzle was 125 °C. The nozzle standoff distance from the substrate was 10 mm. The powder feed rate was 15g/min and the gun travel speed was 50 mm/s.

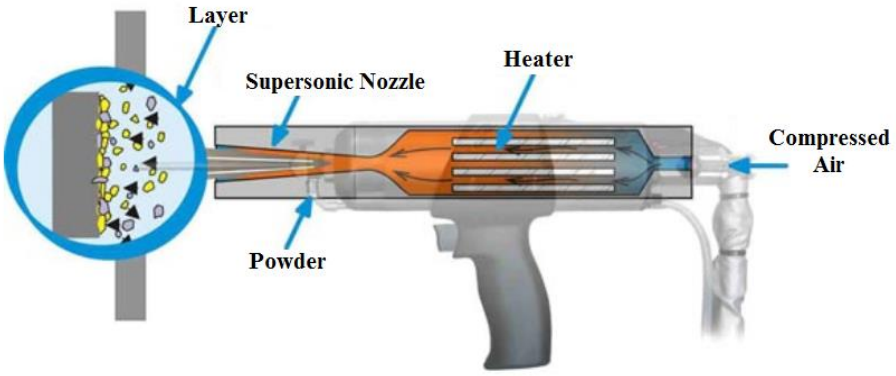

Figure 4.1. Spray metal particles with supersonic into the substrate [103].

Figure 4.2. DYMET 423 Equipment.

4.2. CHARACTERIZATION

4.2.1. SEM

(Carl Zeiss Ultra Plus Gemini Fesem SEM) was used to study the microstructure of the coatings. For the cross-section microstructures of the coatings, samples were prepared metallographically. The coatings' polished cross-sections were etched with 5% Nital reagent. Image analysis was used to determine the porosity and particle size. The values were averaged from over ten SEM pictures taken at random on the coating.

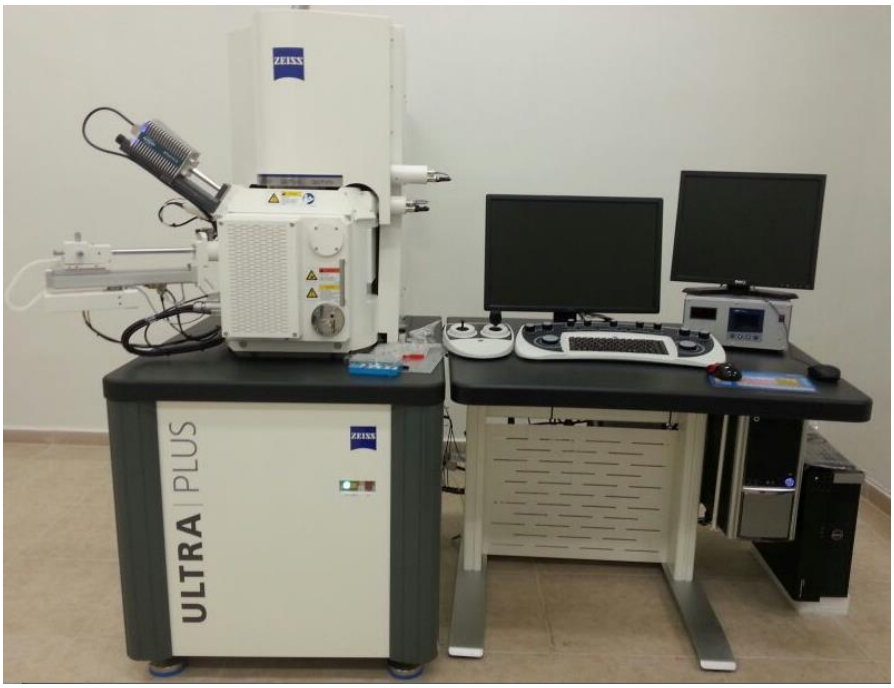

Figure 4.3. Carl Zeiss Ultra plus Gemini Fesem SEM.

Coating thicknesses were measured using the (ASTM B487) standard by Nikon Eclipse MA200 inverted materials microscope with (Clemex Vision PE) Image Analysis Software. The (Nikon ShuttlePix P-400R) was used to photograph the coating surface of the bent specimens.

Figure 4.4. Nikon Eclipse MA200 inverted materials microscope.

Figure 4.5. Nikon ShuttlePix P-400R digital microscope.

4.2.2. Hardness Measurements

Hardness measurements were performed on the surface and the cross-section of the coatings using a QNESS Q10 A+ Vickers hardness tester under the indentation load of 200 g. The stated hardness values are the average of all measurements taken on the relevant samples. At least five measurements were done on the cross-section of the samples. When choosing the hardness measurement spots, the coating surface and coating/substrate contact were avoided.

4.2.3. Bending Test

Three-point bending tests with the universal test machine (Zwick/Roell Z600) were used to study the effects of matrix material on the interface and coating ductility using (ASTM E855-21) standard. Samples were bent up to 60˚ 120˚ 180˚ (± 2) bending angles to compare bending behaviors. The coating's outer surface and side section photographs were inspected after it was bent.

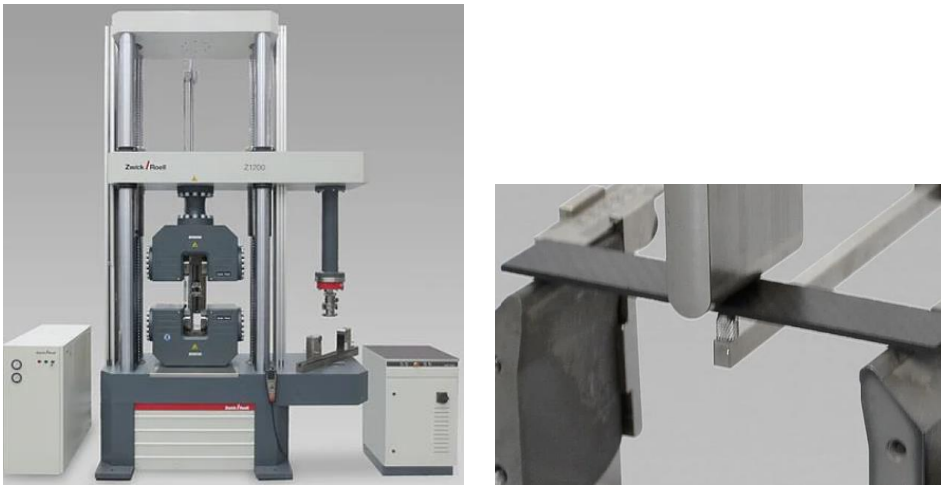

Figure 4.6. Zwick/Roell Z600 Bending test machine.

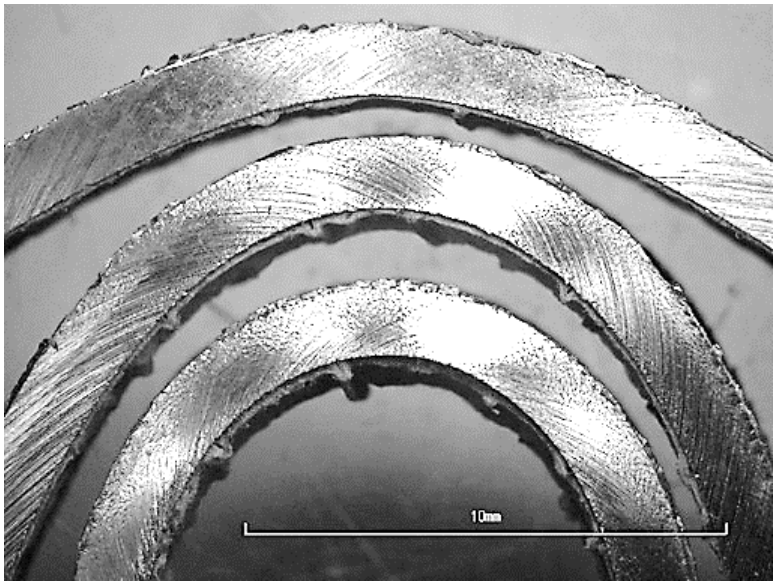

Figure 4.7. Bending material, with different angels, 60°, 120°, and 180°.

4.2.4. Wear Tests

A UTS T10 tribometer was used to study the coatings' tribological behavior under dry sliding conditions at room temperature. The (ASTM G133) standard was used to conduct the tests, which used the ball-on-disc method. The sliding speed was 100 mm/s and the distance was 200 m. 2N, 4N, and 6N were chosen as the applied loads. Another brief wear test was conducted with the same settings as the previous one, but with a 5N load and a 30m distance. A 6 mm ball made of 52100/100Cr6 bearing steel was used as the counterpart material (about 800 HV). The coefficient of friction and the wear dept were reported simultaneously during each test. To assess the wear rate, weight was measured with (Kern ABJ 220) (0.1 mg sensitivity) before and after the wear test. A surface profilometer was used to measure wear scar profiles and coating surface roughness (Mitutoyo SJ-410 Series). The average wear area and consequent wear rate were calculated using six wear scar profiles.

Figure 4.8. UTS T10 tribometer wear test machine.

Figure 4.9. Mitutoyo SJ-410 Series surface profilometer.

4.2.5. Scratch Tests

Scratch tests were used to determine the abrasion resistance of composite samples using a Scratch tester (BRUKER UMT-2-SYS - Kastamonu University Laboratory). A Rockwell-C diamond indenter tip scratched a surface in ambient air at room temperature under a constant load of 1 N at a velocity of 0.0013 mm/sec and a scratch length of 2 mm. During the scratching test, the instantaneous normal force (F_z), tangent force (F_x), tip depth, and friction coefficients were measured.

Figure 4.10. (BRUKER UMT-2-SYS) Scratch tester machine.

PART 5

RESULTS AND DISCUSSIONS

5.1. MICROSTRUCTURE OF LPCS COATINGS

Figure 5.1 shows photos taken from the surfaces of the coated samples. The matrix and reinforcing phase Al_2O_3 particles make up the majority of the coatings that are produced. Al_2O_3 particles may be seen with their sharper and smoother surfaces in the detail view shown in Fig 5.1.a. The powders were severely damaged in the coating with the matrix material Tin (Fig 5.1.d), and the particles were embedded in the matrix, as observed in EDX mapping. The presence of significant Al and O concentrations in Al_2O_3 particles embedded in the matrix distinguishes them. In the coating with zinc matrix (Fig. 5.1b), however, the powders left on the top surface are less distorted under similar production conditions. However, the distortion is considerable in the lower regions of the coating, as shown in cross-sectional views in Figure 5.2.b. The peening effect causes coating densities to drop from the substrate material to the upper surface. Certain proportions of metal-ceramic mixtures have been shown to improve deposition efficiency over metallic powders alone [27,28].The amount of Al_2O_3 employed in the coating is roughly 40-50 percent lower than the feedstock powder, as shown in the surface images (Figure 5.1) and side section views (Figure 5.2) of all coatings. According to other research, a considerable portion of the ceramic powder utilized in the coating procedure did not pass through the coating [132]. Because of their structure, most Al_2O_3 particles escape the coating without binding when they collide. Only when embedded in matrix particles or enclosed between them m ay they be incorporated in the coating [22,80]. Even though not all of the Al_2O_3 particles used in production are transported to the coating material, the pinning effect makes the percentage of Al_2O_3 in the mixture crucial. The absence of pore development in the coatings generated in this investigation implies that the matrix/ Al_2O_3 employed was adequate.

A1

A2

A3

A4

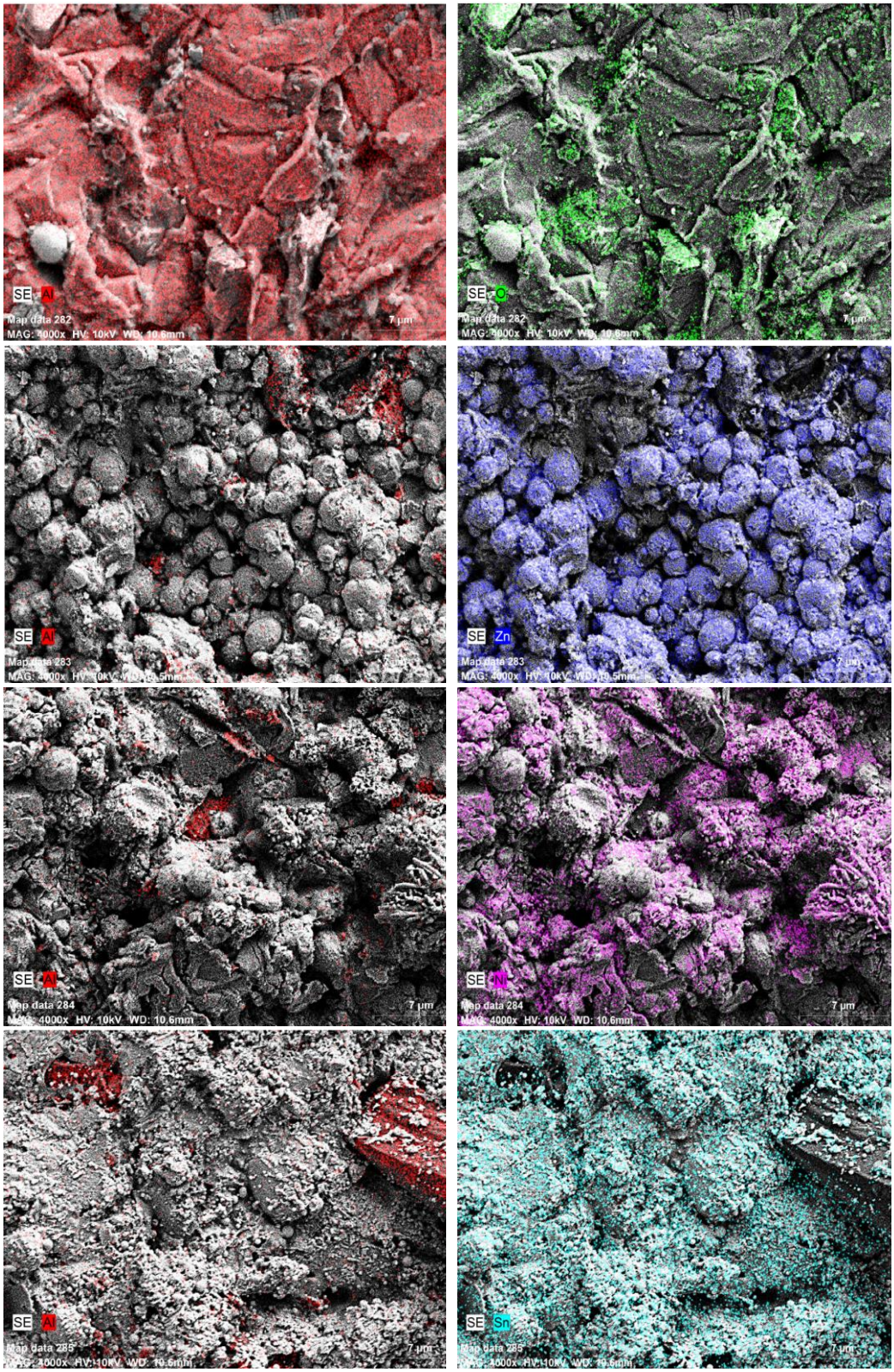

Figure 5.1. Surface images of the coated samples respectively A1, A2, A3 and A4.

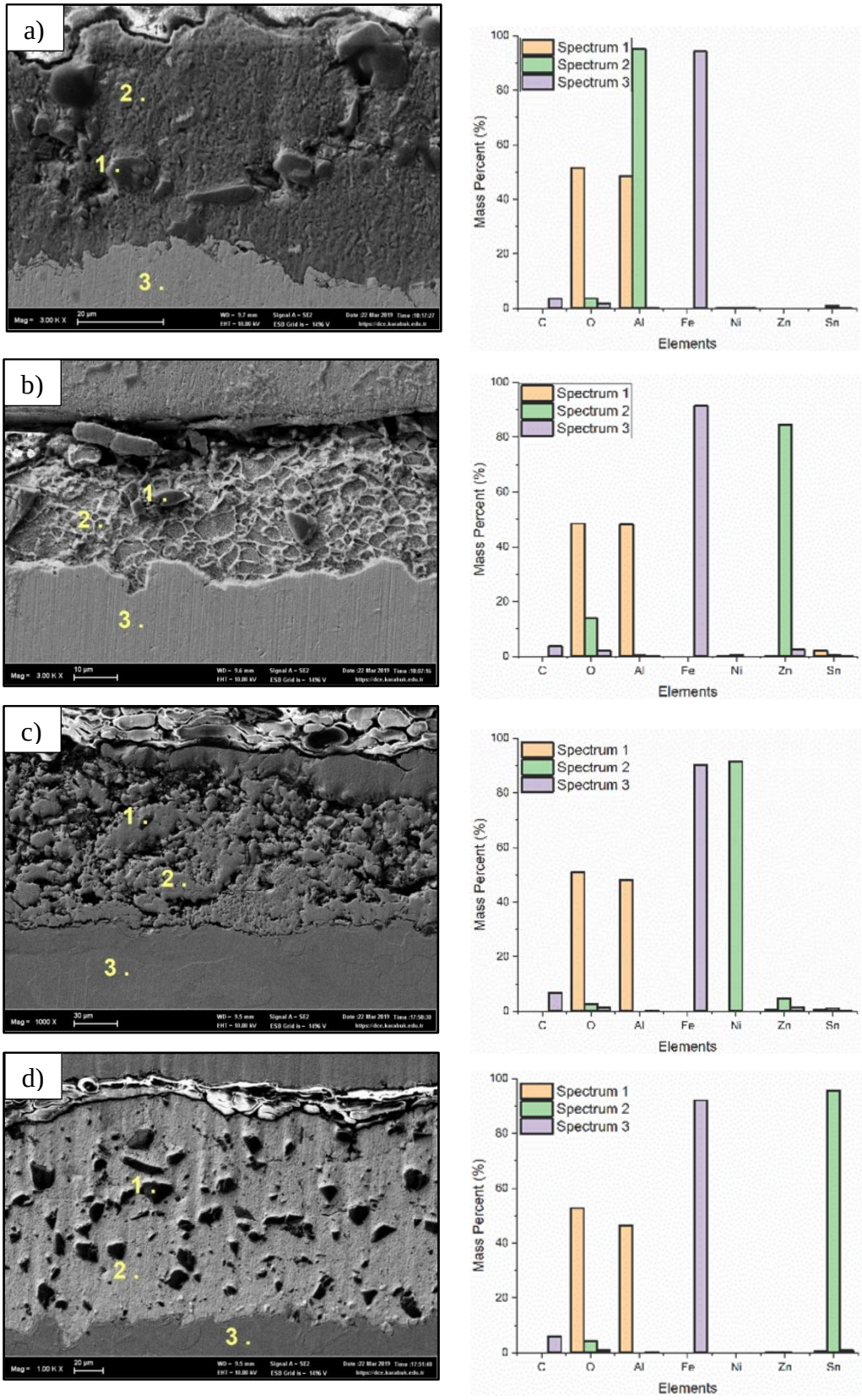

Figure 5.2. Side section views of all coatings and point EDX analyses a) A1, b) A2, c) A3 and d) A4.

Since each component has a different relative deposition impact, the actual volume fraction deposited in two-phase powder mixes is usually not the same as the feedstock powder. The amount of particles that passed through the coating was estimated to be roughly 10-15% based on cross-sectional studies. The hammering impact of the non-deformable Al_2O_3 particles boosts the coating's bonding ability and density, hence the number of Al_2O_3 particles is critical. However, a study found that a high Al_2O_3 ratio had a detrimental effect on the coating because it increased particle interaction and that a 15 percent Al_2O_3 ratio gave the most efficient deposition [132].

When all of the coatings' cross-sectional pictures (Figure 5.2) were analyzed, no big pores were detected in any of the samples. Furthermore, the Al_2O_3 particles in the coatings have a fairly homogeneous distribution, showing that the powders do not separate in the gas flow under the spray circumstances used. In the Al matrix coating shown in Figure 5.2a, few tiny porosities were found between adjacent Al_2O_3 particles. Sample A3 (Ni + Al_2O_3), on the other hand, has a more heterogeneous structure (Fig.5.2c). In comparison to other coatings, this one includes less alumina particles and has more defined micropores and microcracks.

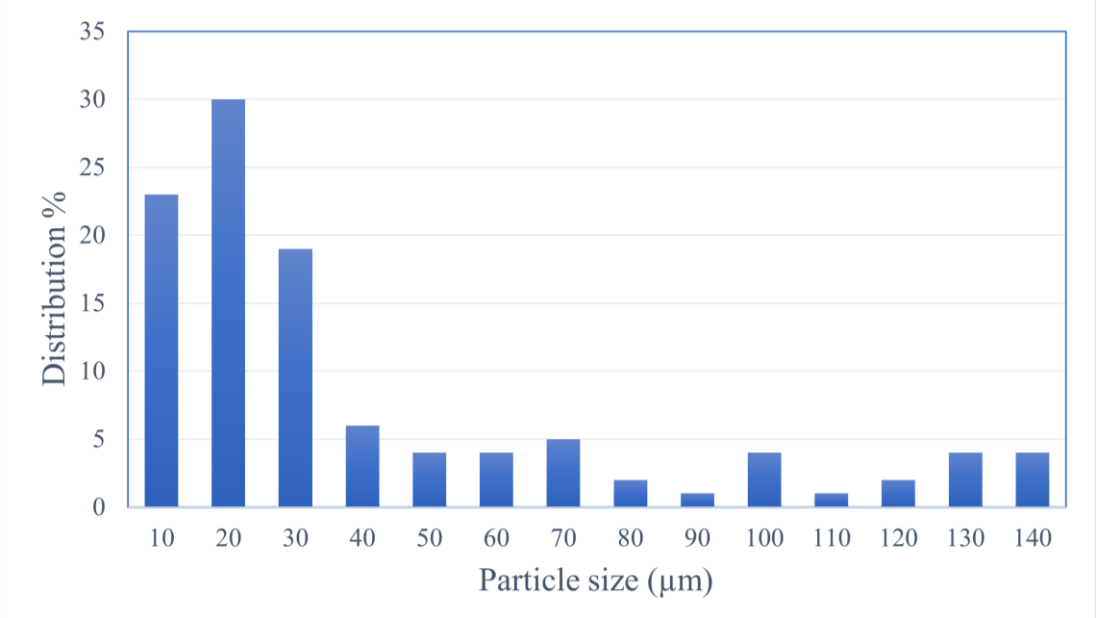

Figure 5.3. Al_2O_3 particle size distribution.

In a research using identical materials, comparable findings were also observed [133]. Because Ni is harder than other matrix powders at similar coating settings, it has been claimed that bonding ceramic particles is problematic. All coatings, on the other hand, are applied with the same parameters, and it is considered that this is due to the higher melting temperature and strength of Ni particles. Greater plastic deformation causes the coating to have less porosity at low spraying temperatures compared to the melting temperatures of the matrix particles.

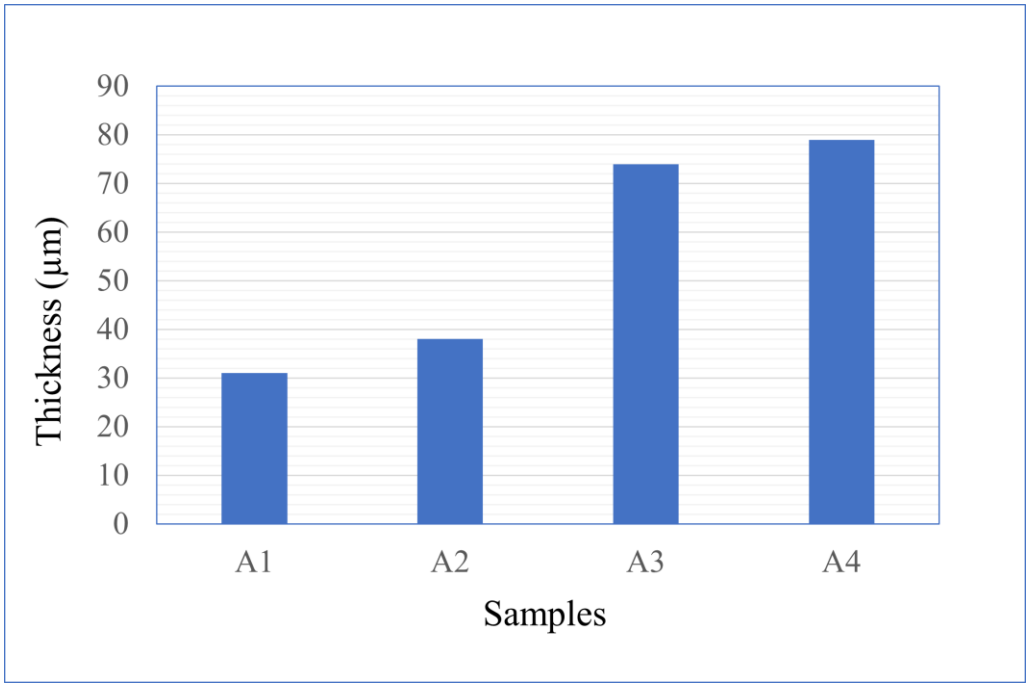

Figure 5.4. Average coating thickness.

Figure 5.3 shows the average size distribution of Al_2O_3 particles incorporated in the coating. Different sizes of ceramic powder have been shown to produce variations in particle velocity and kinetic energy. Their simulations revealed that as particle size grew, velocity dropped but kinetic energy rose noticeably [134]. This has an impact on the coating's bonding behaviour. In cold spray deposition, there are two forms of bonding: particle-to-substrate bonding, which is necessary for the development of the initial layer of the coating, and particle-to-particle bonding, which is used to thicken the coating. Matrix particles were bonded primarily by intense plastic deformation and mechanical interlocking.

5.2. MECHANICAL PROPERTIES OF CS COATINGS

5.2.1. Roughness Test

Surface roughness is also influenced by particle size and distribution in the coating. Wang et al. investigated the impact of ceramic particle size on coating surface roughness and found that the coating surface roughness rises with particle size [135]. Figure 5.5 shows the surface roughness graphs and average coating values.

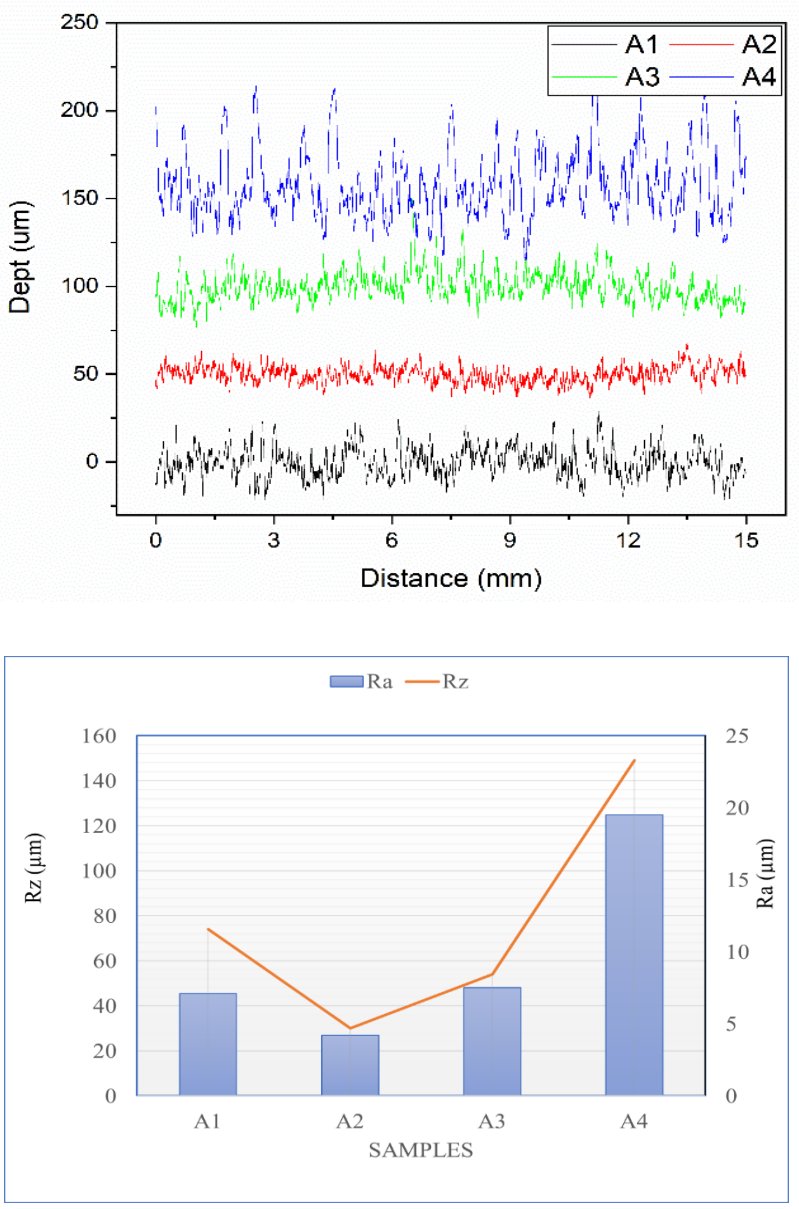

Figure 5.5. Surface roughness of coatings.

The A2 coating had the lowest average roughness (R_a) and the smallest differential (R_z) between the max and min roughness. While A1 and A3 have values that are close to A2, A4 coating has the largest difference and average roughness values.

5.2.2. Hardness Test

Figure 5.6 shows the average hardness values measured from the cross-section of the coatings. Al_2O_3 has high microhardness, wear resistant, and chemically stable material. As a consequence, the hardness and tribological behaviour of the coatings were directly impacted by the difference in Al_2O_3 transition. Particles with a high kinetic energy undergo substantial plastic deformation, resulting in work hardening. As a result, cold spray metal coatings are predicted to have a substantially greater hardness than comparable annealed cast material[136,137].

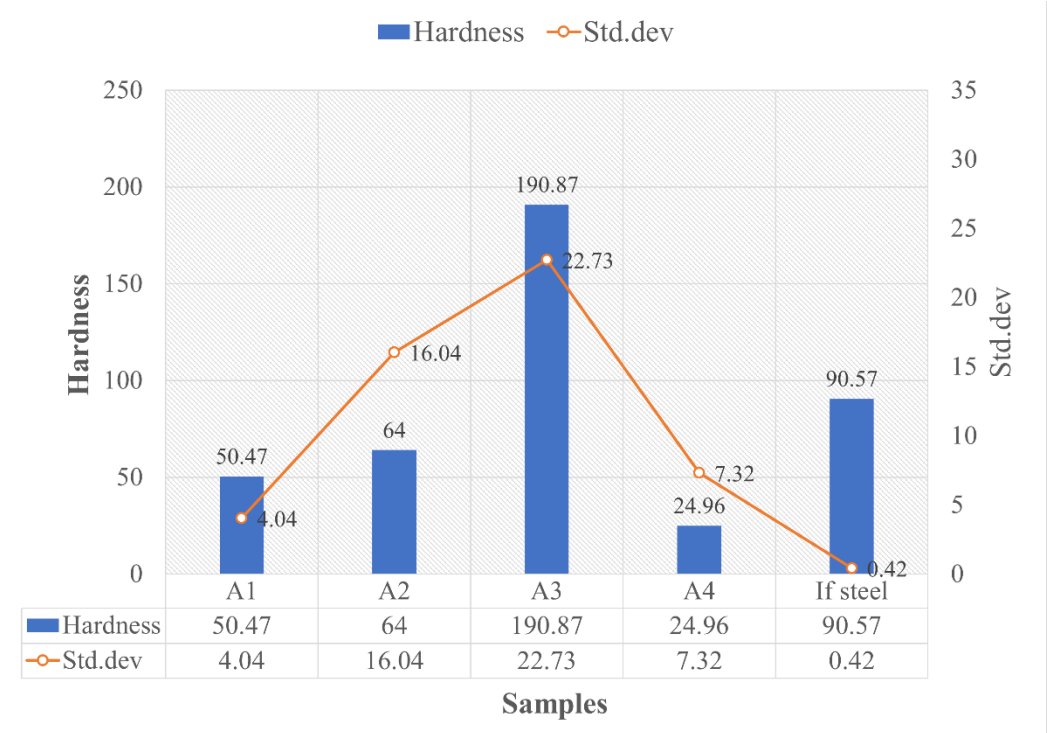

Figure 5.6. Average hardness values of coatings and substate.

When comparing hardness levels, it's clear that the coating's matrix material is the most important factor. The coating with the Sn matrix was the softest, as predicted, whereas the coating with the Ni matrix was the toughest. Only the Ni+ Al_2O_3 coating, on the

other hand, is tougher than the base material (IF-steel). This is expected to give a wear resistance benefit.

5.2.3. Bending Test

The various matrices employed in the coating have an impact on the coating's bonding, ductility, and hardness. A three-point bending test was done at various angles to assess this impact. Only noticeable fractures on the surface of the A2 coating were discovered when the bent surfaces were inspected (Figure 5.7). The A1 and A3 coatings' face-centered cubic structure proved able to withstand deformation. The soft and ductile nature of A4 on the other hand, inhibited fracture development. Also bendable are these three coating materials. However, the A2 covering was brittle at room temperature and could not withstand bending deformation.

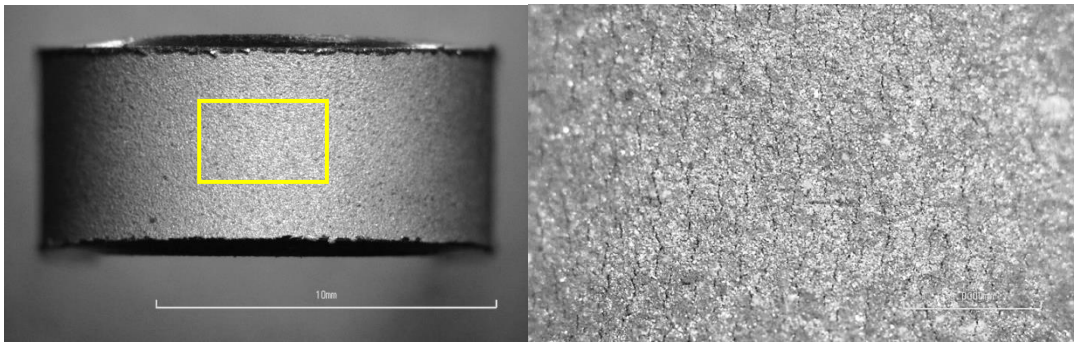

Figure 5.7. Surface view of A2 sample after 180˚ bending test.

Higher magnification investigations of the deformed particle shape from the side section of bent specimens (Figure 5.8) indicate where the matrix particles are separated at their interface. The glare in Figure 5.8a reveals the existence of the oxide and hence the crack's location. Although fractures are most commonly visible between ceramic particles, they can also be visible between the coating and the substrate in some cases.

Even though there are no apparent fractures on the coating surface, as in A4, microstructural studies reveal flaws on the interior of the coating. These fissures usually appear between the matrix and the particle, or even between the particles themselves. Figure 5.8b also shows how the ductile matrix absorbs and stops those

cracks. As a result, the lack of visible fractures open to the outside is beneficial to corrosion resistance.

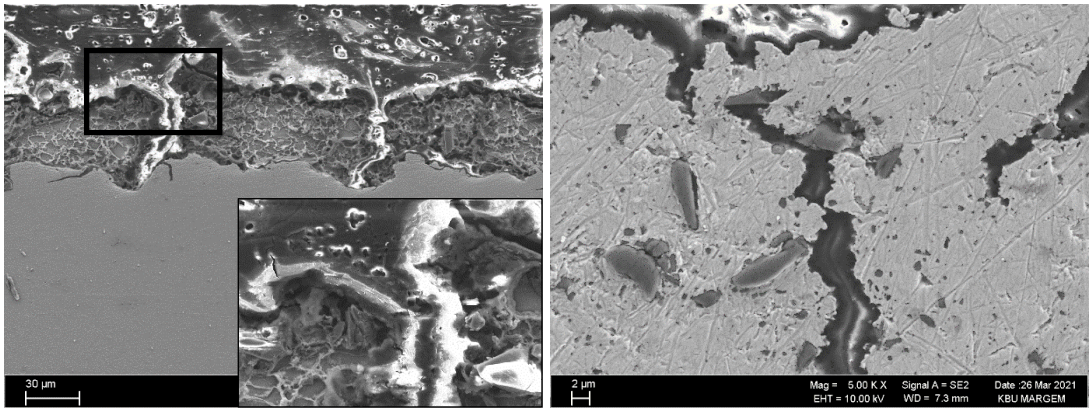

Figure 5.8. Cross-section view of A2 and A4 samples after 180˚ bending test.

5.2.4. Wear Test

The coated samples were subjected to abrasion tests at various weights and distances. Figure 5.9 and Figure 5.10 shows the traces and losses from a dry abrasion test with a 5N load and a 30m distance. When the trace depths and volume losses were evaluated, the A4 coating suffered was the most loss, while the A2 coating suffered was the least.

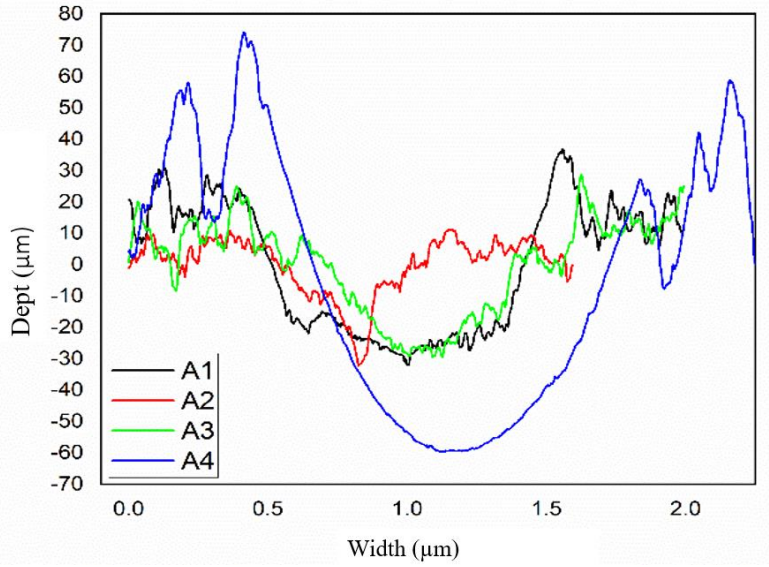

Figure 5.9. The values of wear depths from the 30m, 5N wear test.

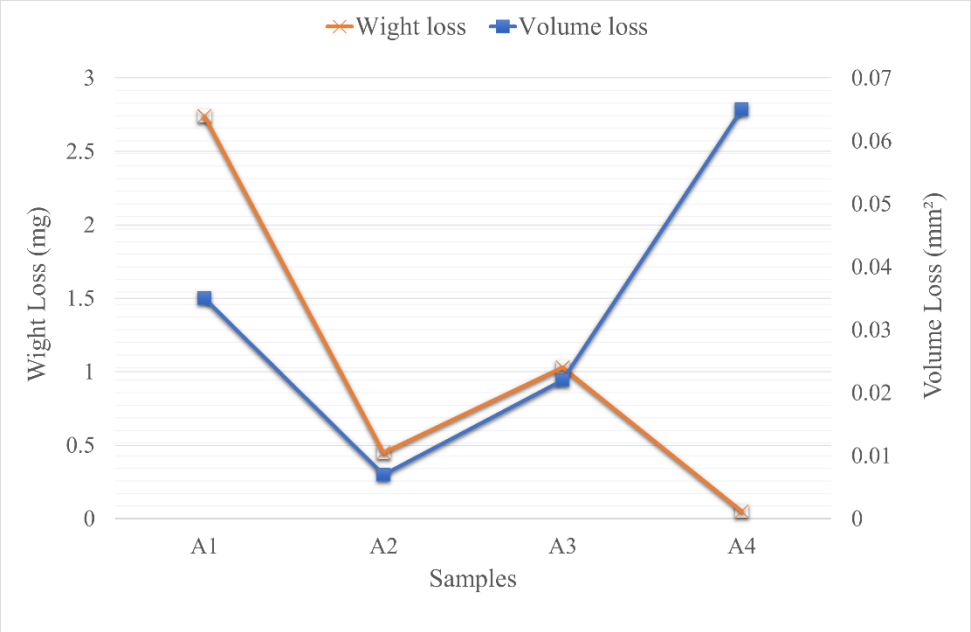

Figure 5.10. The values of loss amounts resulting from the 30m, 5N wear test.

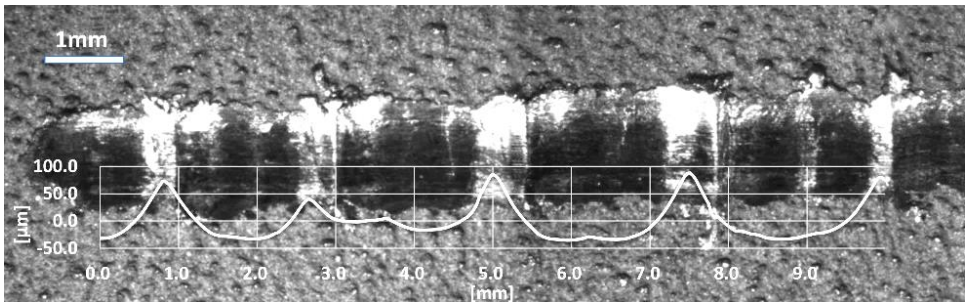

Figure 5.11. Worn trace image and surface profilometry of A4 coating.

A different scenario was discovered when the weight losses (Figure 5.10) measured as a result of the identical wear tests were investigated. Although the changes in A1, A2, and A3 were similar, the amount of weight loss observed in A1 was greater than the others. The sort of wear products generated is the major cause for this variance. The abrasion of A1 resulted in the formation of more tiny particles than the other two coatings, as shown in the wear surface studies (Figure 5.12a). Another significant difference is that the A4 coating has the highest amount of volume loss, but the weight loss measured in the same sample is nearly nil. Figures 5.10 and 5.12d show how plastic deformation of the covering created this condition. Friction distorted the coating, yet the worn coating did not break; instead, it piled locally.

Figure 5.12 shows an example of a trace picture generated after wear. Due to its high Al_2O_3 concentration and oxidation potential, A1 tends to collapse. This test did not reveal the development of a coating or protective interlayer, which is common at the Al-Steel wear contact. Furthermore, there was no smearing or adhesions on the ball during the abrasive ball surface evaluations (Figure 5.13a). Instead, tiny scratches are observed as a result of hard particles that are comparable to the worn surface.

The combination of these (A1) coating powders has the most Al_2O_3, and the effect of the particle in the coating on wear resistance is high, as predicted. The type, size, and distribution of the reinforcing phase determine the wear resistance of a composite. It has been notes that the addition of ceramic particles to 7075 Al powder has been found to increase the wear performance of cold spray coatings substantially [138]. Furthermore, it has been shown that when the Al_2O_3 ratio of pure Al - 25% Al_2O_3 composite coating is 75 %, the wear rate is reduced by more than five times [22].

There is overall rubbing as well as localized chipping seen on the A2 worn surface (Figure 5.12.b). The smearing that results may also be seen on the abrasive Steel ball surface (Figure 5.13b). The inclusion of a Zn- Al_2O_3 coating has been shown to lower the friction coefficient of mild steel substrates [139]. They discovered that alumina particles in the Zn matrix function as lubricants, decreasing the amount of direct contact between the alumina stylus ball and the metal matrix. The lowest wear coefficient value was recorded in this coating following the Sn, which is immediately deformed, in the change in coefficient of friction shown in Figure 5.14. The change in friction coefficient is also more stable than the other coatings. This confirms the formation of a protective intermediate layer.

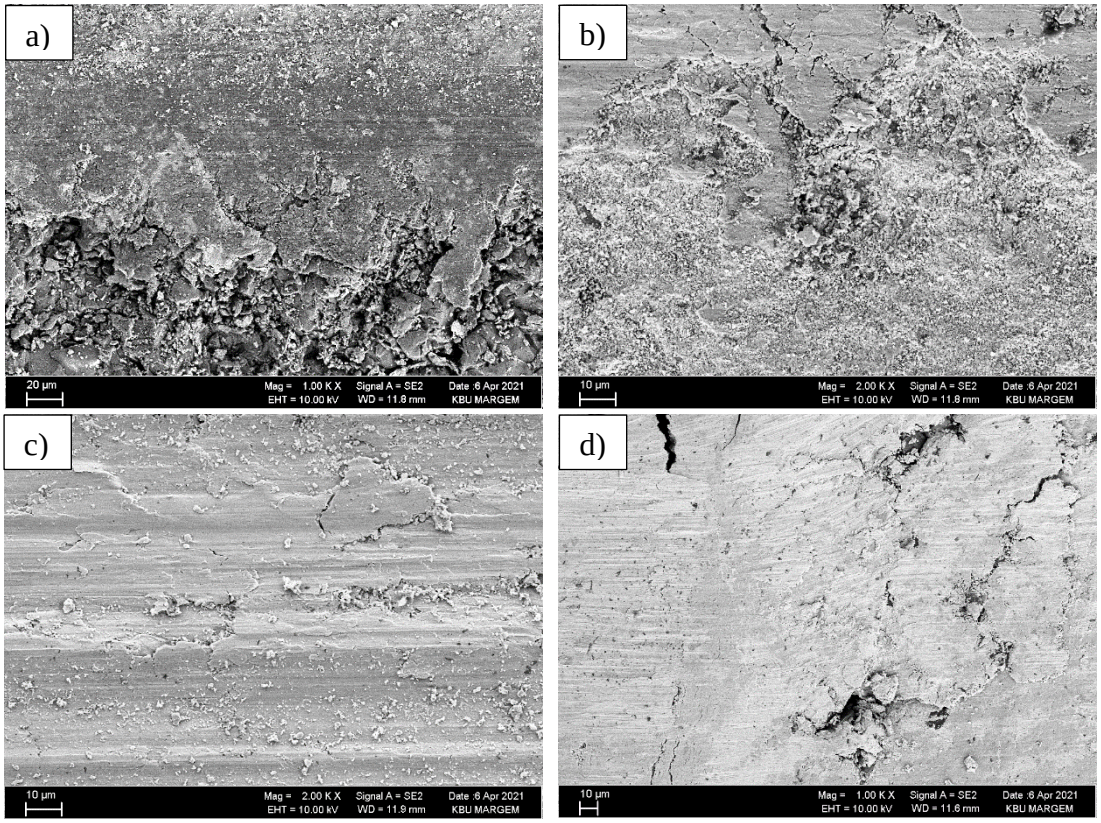

Figure 5.12. Worn surface images of a)A1, b)A2, c)A3 and d)A4 coatings.

Plastic deformation and smearing, as well as a minor amount of chipping, can be seen in the wear marks of the Ni-matrix coating (Fig. 5.12c). Partial ruptures were seen in several locations. The Ni coating on the Al_2O_3 particles was torn, and ceramic particles remained in the pits, according to the map EDX analysis (fig. 5.14a) done in one of these locations. This might be because the connection between Ni- Al_2O_3 is weaker than the one between Ni-Ni [140].As a result, the Al_2O_3 particles' thin Ni areas are more readily detached from the coating or damaged.

The Ni-matrix coating had a low wear rate, whereas the abrasive ball had a high adhesion rate (Figure 5.13c). The abrasive steel ball's strong affinity and the advantageous cubic structure likely aided Ni adherence to the surface. Because the number of active sliding systems in the Zn matrix coating is inadequate, plastic deformation is predicted to be facilitated when temperature rises owing to friction. As a result, the Zn matrix layer and the abrasive steel ball are more likely to form a weaker connection. This is the reason why the Ni coating has a greater friction coefficient than the others.

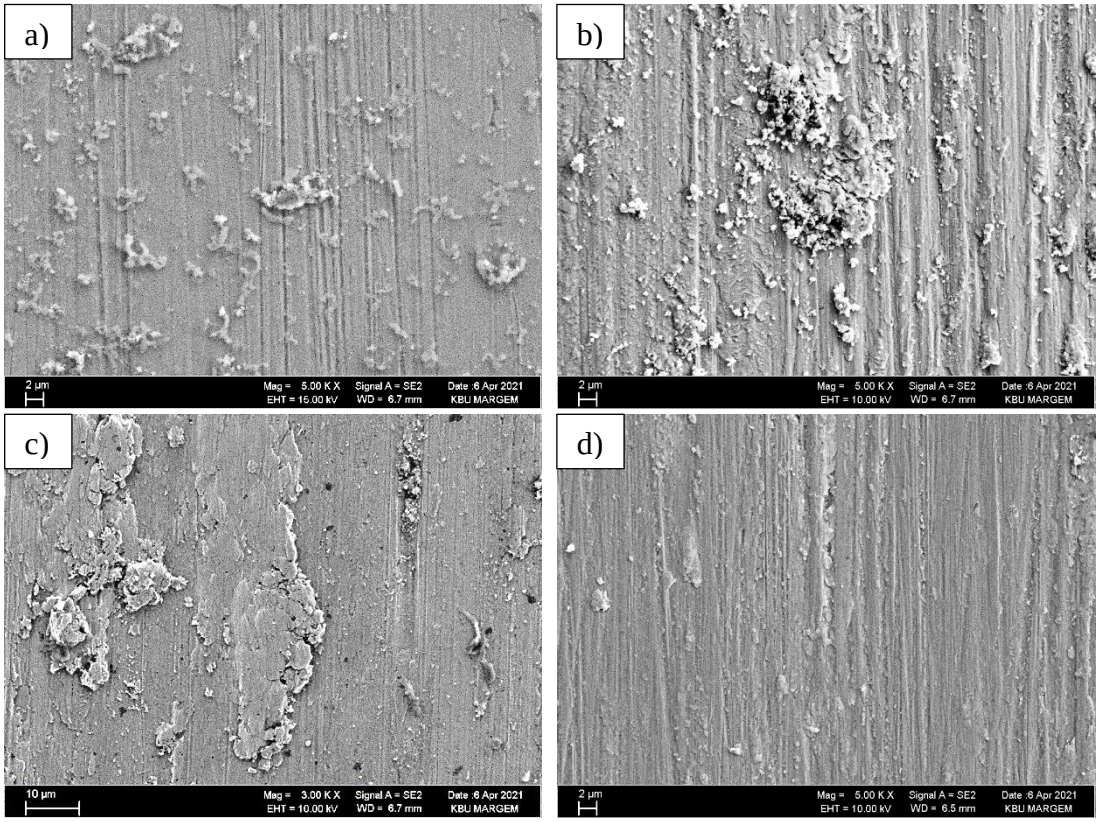

Figure 5.13. Surface view of abrasive steel ball after wearing of a)A1, b)A2, c)A3 and d)A4 coatings.

Due to the poor strength and hardness of the matrix, the Sn matrix coating (A4) was extensively distorted, crushed, and localized agglomerations were detected during wear (Figure 5.12d).

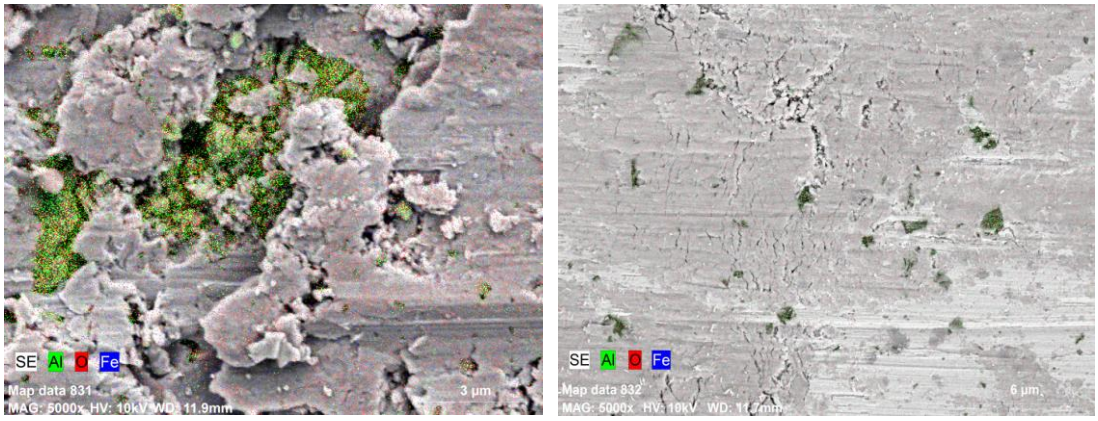

Figure 5.14. EDX map analysis on wear surfaces of a) A3 and b) A4 coatings.

SEM and map EDX (Figure 5.14b) studies carried out at high magnification on these mounds indicated the formation of tiny fractures, which are typically produced by Al_2O_3 in the structure. Adhesion was not found on the steel ball utilized in the wear of this coating (Figure 5.13d), but tiny scratches on the surface were noticed owing to the ceramic particle reinforcement.

5.2.5. Scratch Tests

Scratch tests with 1N constant load were done to assess the binding strengths and fracture processes of the matrix materials of the coatings, and the friction coefficient versus time graphs of the coated samples are shown in Figure 5.15. For all coatings, relatively low friction behaviour were found for coated samples. From A1 to A4, the mean coefficient of friction (CoF) values of coated samples were 0.427, 0.388, 0.434, and 0.379, respectively. The values of the friction coefficient curves showed variations when they were studied. In this case, hard thin coatings were shattered, forming wear debris as a result of the abrasive action. The Sn coated specimens had the lowest friction coefficient values.

The friction coefficient, F_x, F_z forces, and C_p were also measured along with the friction coefficient. The coefficient of friction is determined by the resistive force (F_x), which produces a similar graph. The hard phases varied owing to agglomeration or rupture and differed somewhat from the change in the coefficient of friction, thus the normal load (F_z) was not continuous 1N as determined.

In general, the friction coefficients are similar in A1 and A3, while A3 shows greater reductions. These dips are most likely caused by flaws in the coating. In A2, there was a very steady change in the coefficient of friction, which may be explained in terms of the coating wear characteristics. At the first, the friction coefficient of A4 rose, most likely owing to plastic deformation. After that, it took a regular path. In scratch tests, other coatings' scratcher tip depths (C_p) steadily rose under constant stress, but the A4 coating's C_p fell considerably at first, then exhibited a steady constant change. The friction coefficient also given a similar change.

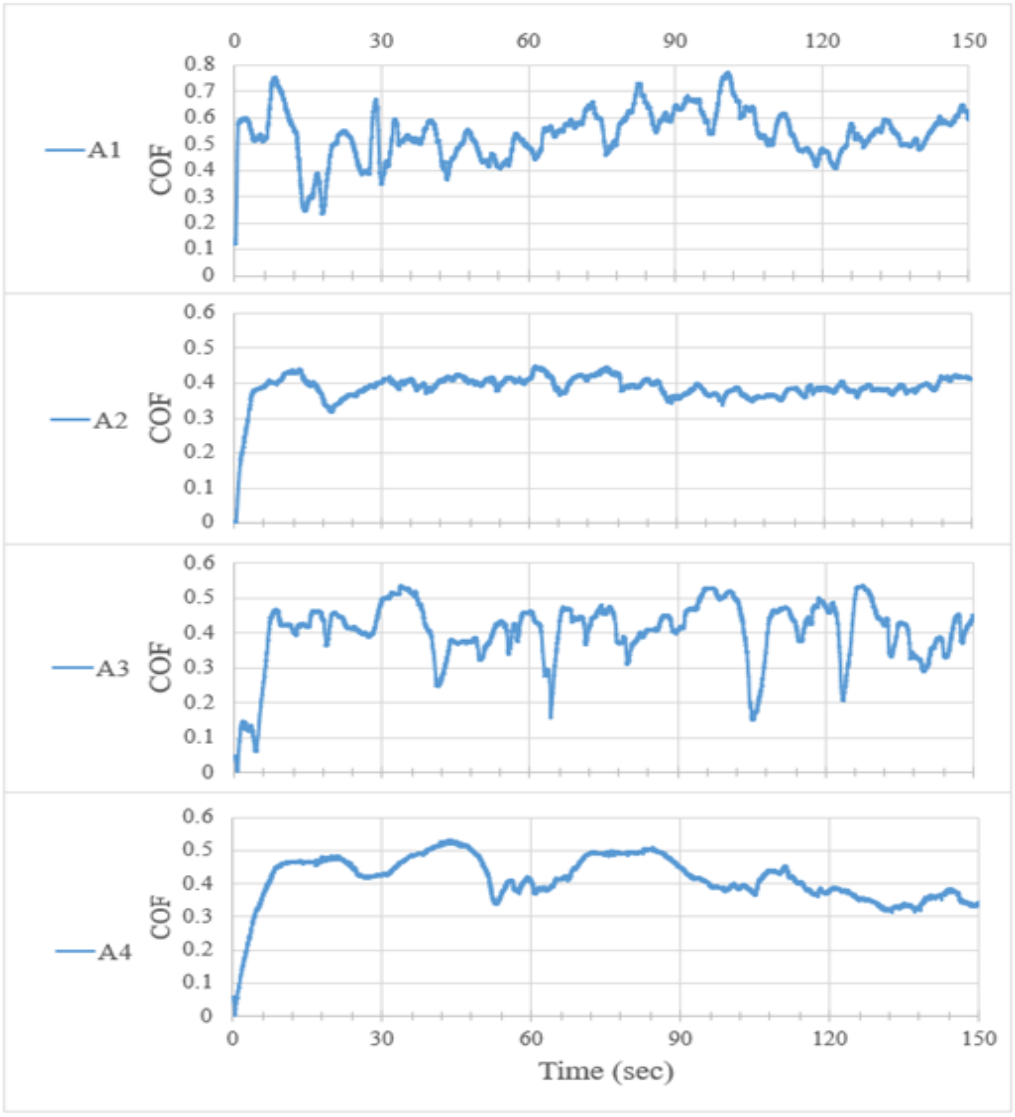

Figure 5.15. Scratch friction coefficients of coated specimens (1N-150 sec).

PART 6

CONCLUSIONS

In this study, Aluminum, Zinc, Nickel, and tin matrix powders, as well as alumina (Al_2O_3) particle powders, were effectively coated on EN 10130 steel using the low-pressure cold spray (LPCS) to generate particle reinforced composite coatings. The ceramic particles that collided with the base material cleaned and roughened the surface, allowing for excellent bonding and generating a peening effect on the metal powders.

The gaps and cracks between the particles were particularly noticeable in the Ni matrix coating when the coated portions were inspected. Other coatings exhibit comparable characteristics and are in nearly excellent condition, with the exception of a few micropores. Only approximately 15% of the ceramic powders were transported to the coating, as predicted, because the metal/ceramic ratio in the powder combination did not occur in the coatings. This ratio, however, was found to be adequate.

Different roughness rates have occurred depending on the physical characteristics of the matrix powders on the coated surfaces and the Al_2O_3 flowing into the matrix. The average roughness (R_a) values were calculated from lowest to highest for A2, A1, A3, and A4 coatings, respectively.

A comparable alteration in terms of pits and bumps that occur at regular intervals in Al (A1) and Ni (A3) matrix coatings with identical crystal lattice structures was noticed as a consequence of the scratch test performed on the coating surfaces. In comparison to A1 and A3, the friction coefficient of Zn (A2) matrix coating is lower, with modest positive variations in general. As observed in the traces generated as a consequence of abrasion tests on the Sn (A4) matrix coating, localized agglomerations

caused variations at lengthy intervals, while a near-smooth transition occurred in other regions.

Coating hardness was determined from high to low for A3, A2, A1, and A4 coatings, respectively. The amount of volume loss has been calculated as A2, A3, A1, and A4, correspondingly, from low to high, respectively. As a result of wear tests done at various weights and distances. The unexpected case was found that less volume loss was found in the Zn matrix coating (A2), which has a lower hardness than the Ni matrix coating (A3), as a result of the interface interaction between the coating and the abrasive and the lubricating effect,

The only coating that developed obvious cracks following bending tests was the Zn matrix coating, which was brittle in the studied parameters and could not withstand bending deformation. The most detrimental factor for this coating was discovered to be plastic forming.

As a result, among the four metals employed, Zn was found to be the best-suited matrix material, taking into account the coating quality, which affects corrosion resistance, wear resistance and cost.

REFERENCES

1. Hoile, S., "Processing and properties of mild interstitial free steels" ***Materials Science and Technology,*** 16(10): 1079-1093 (2000).

2. Gupta, A. K., & Kumar, D. R., "Formability of galvanized interstitial-free steel sheets", ***Journal of Materials Processing Technology,*** 172(2): 225-237 (2006).

3. Liang, Y. L., Wang, Z. B., Zhang, J. B. & Lu, K., "Formation of interfacial compounds and the effects on stripping behaviors of a cold-sprayed Zn–Al coating on interstitial-free steel", ***Applied Surface Science,*** 3(40): 89-95 (2015).

4. Gupta, A. K., & Kumar, D. R., "Formability of galvanized interstitial-free steel sheets", ***Journal of Materials Processing Technology,*** 172(2): 225-237 (2006).

5. Kenter, J. O., O'Brien, L., Hockley, N., Ravenscroft, N., Fazey, I., Irvine, K. N. & Williams, S., "What are shared and social values of ecosystems?", ***Ecological Economics,*** 11(1): 86-99 (2015).

6. Tachibana, K., Morinaga, Y., & Mayuzumi, M., "Hot dip fine Zn and Zn–Al alloy double coating for corrosion resistance at coastal area", ***Corrosion Science,*** 49(1): 149-157 (2007).

7. Shih, H. C., Hsu, J. W., Sun, C. N., & Chung, S. C., "The lifetime assessment of hot-dip 5% Al–Zn coatings in chloride environments", ***Surface and Coatings Technology,*** 150(1): 70-75 (2002).

8. Xu, B., Phelan, D., & Dippenaar, R., "Role of silicon in solidification microstructure in hot-dipped 55 wt% Al–Zn–Si coatings", ***Materials Science and Engineering: A,*** 473(2): 76-80 (2008).

9. Kosarev, V. F., Klinkov, S. V., Alkhimov, A. P., & Papyrin, A. N., "On some aspects of gas dynamics of the cold spray process", ***Journal of Thermal Spray Technology,*** 12(2): 265-281 (2003).

10. Leonardi, F., Ginder, J. M. and McCune, R. C., "Method of manufacturing electromagnetic devices using kinetic spray," ***US Patent 7,097,885,*** Washigton, USA, 12-18 (2006).

11. Ito, K., Ogawa, K. and Shoji, T. "193 Deposition mechanisms of low pressure type cold spray coatings", ***Proc. Conf. Tohoku Branch,*** 2007(42): 183–184 (2007).

12. Ogawa, K., Ito, K., Ichimura, K., Ichikawa, Y., Ohno, S., & Onda, N.,

"Characterization of low-pressure cold-sprayed aluminum coatings", ***Journal of Thermal Spray Technology,*** 17(6): 728-735 (2008).

13. Grujicic, M., Saylor, J. R., Beasley, D. E., DeRosset, W. S., & Helfritch, D., "Computational analysis of the interfacial bonding between feed-powder particles and the substrate in the cold-gas dynamic-spray process", ***Applied Surface Science,*** 219(4): 211-227 (2003).

14. Assadi, H., Gärtner, F., Stoltenhoff, T., & Kreye, H., "Bonding mechanism in cold gas spraying", ***Acta Materialia,*** 51(15): 4379-4394 (2003).

15. Gray, J., & Luan, B., "Protective coatings on magnesium and its alloys—a critical review", ***Journal of Alloys and Compounds,*** 336(2): 88-113 (2002).

16. Wei, Z. S., Liu, L., & Ding, W. J., "Al arc spray coating on AZ31 Mg alloy and its corrosion behavior", ***In Materials Science Forum,*** 48(8): 685-688 (2005).

17. Garcia, I., Fransaer, J., & Celis, J. P., "Electrodeposition and sliding wear resistance of nickel composite coatings containing micron and submicron SiC particles", ***Surface and Coatings Technology,*** 148(3): 171-178 (2001).

18. Chen, X. H., Cheng, F. Q., Li, S. L., Zhou, L. P., & Li, D. Y., "Electrodeposited nickel composites containing carbon nanotubes", ***Surface and Coatings Technology***, 155(3): 274-278 (2002).

19. SzczygieI, B., & KoIodziej, M., "Composite Ni/Al {sub 2} O {sub 3} coatings and their corrosion resistance", ***Electrochimica Acta,*** 50 (2): 334-466 (2005).

20. Arafa, I. M., & Al-Atrash, M., "Synthesis and characterization of diaminecarbosilazane-containing polymers", ***Journal of Macromolecular Science, Part A,*** 39(12): 1475-1486 (2002).

21. Erler, F., Jakob, C., Romanus, H., Spiess, L., Wielage, B., Lampke, T., & Steinhäuser, S., "Interface behaviour in nickel composite coatings with nano-particles of oxidic ceramic", ***Electrochimica Acta,*** 48(22): 3063-3070 (2003).

22. Vo, P., Goldbaum, D., Wong, W., Irissou, E., Legoux, J. G., Chromik, R. R., & Yue, S., "Cold-spray processing of titanium and titanium alloys. In Titanium Powder Metallurgy", ***Butterworth-Heinemann,*** Germany, 405-423 (2015).

23. An, J., Li, R. G., Chen, C. M., Xu, Y., Chen, X., Guo, Z. X., & Liu, Y. B., "Comparative studies on wear behaviour between as cast AZ91 and Mg97Zn1Y2 magnesium alloys", ***Materials Science and Technology,*** 23(10): 1208-1214 (2007).

24. Connolly, B. J., Deffenbaugh, K. L., Moran, A. L., & Koul, M. G., "Environmentally assisted crack growth rates of high-strength aluminum alloys", ***JOM,*** 55(1): 49-52 (2003).

25. Hassani-Gangaraj, S. M., Moridi, A., & Guagliano, M., "Critical review of corrosion protection by cold spray coatings", ***Surface Engineering,*** 31(11): 803-815 (2015).

26. Kieback, B., Neubrand, A., & Riedel, H., "Processing techniques for functionally graded materials", ***Materials Science and Engineering: A,*** 362(2): 81-106 (2003).

27. Wang, M., Tan, G., Ren, H., Xia, A. & Liu, Y., "Direct double Z-scheme Og-C3N4/Zn2SnO4N/ZnO ternary heterojunction photocatalyst with enhanced visible photocatalytic activity", ***Applied Surface Science,*** 49(2): 690-702 (2019).

28. Sova, A., Papyrin, A., & Smurov, I., "Influence of ceramic powder size on process of cermet coating formation by cold spray", ***Journal of Thermal Spray Technology,*** 18(4): 633 (2009).

29. Ralph, B. Yuen, H. C. and Lee, W. B. "The processing of metal matrix composites - An overview", ***J. Mater. Process. Technol.,*** 63(3): 339–353 (1997).

30. Lee, H. Y., Yu, Y. H., Lee, Y. C., Hong, Y. P., & Ko, K. H., "Cold spray of SiC and Al 2 O 3 with soft metal incorporation: A technical contribution", ***Journal Of Thermal Spray Technology,*** 13(2): 184-189 (2004).

31. Internet: Boyle, K. P. "Cold work embrittlement of interstitial-free sheet steel", **https://macsphere.mcmaster.ca/handle/11375/7561**/(2001).

32. Lleweuyn, D.T. and Hudd, R.C., "Steels - metallurgy and applications", ***Oxford: division of Reed Educational and Professional Publishing Ltd,*** UK, 34-56 (2004).

33. Yi, H. L., Sun, L., & Xiong, X. C., "Challenges in the formability of the next generation of automotive steel sheets", ***Materials Science and Technology,*** 34(9): 1112-1117 (2018).

34. Cantergiani, E., "Recherche uO Research: Mechanical Properties of Functionally Graded Materials: Carbon Gradient inside Interstitial Free Steel", ***Master Thesis, Faculty of Graduate and Postgraudte Studies, University of Ottawa,*** Ottawa, Canada, 45-58 (2016).

35. Ko, Y. G., Lee, J. S., "Microstructure evolution and mechanical properties of ultrafine grained IF steel via multipass differential speed rolling", ***Materials Science and Technology,*** 29(5): 553-558 (2013).

36. Ray, R. K., & Ghosh, P., "An overview on precipitation and texture formation in IF and IFHS steels during processing", ***Materials and Manufacturing Processes,*** 25(3): 195-201 (2010).

37. Totten, G. E., Funatani, K., & Xie, L., "Handbook of metallurgical process design", ***CRC Press,*** USA, 23-33 (2004).

38. Hua, M., Garcia, C. I. & DeArdo, A. J., "Precipitation behavior in ultra-low-carbon steels containing titanium and niobium", ***Metallurgical and Materials Transactions A,*** *28*(9): 1769-1780 (1997).

39. Rana, R., Bleck, W., Singh, S. B. & Mohanty, O. N., "Development of high strength interstitial free steel by copper precipitation hardening", ***Materials Letters,*** 61(15): 2919-2922 (2007).

40. Ray, R. K., Ghosh, P., & Bhattacharjee, D., "Effects of composition and processing parameters on precipitation and texture formation in microalloyed interstitial free high strength (IFHS) steels", ***Materials Science and Technology,*** 25(9): 1154-1167 (2009).

41. Shi, J., & Liu, C. R., "Role of nanoscale TiC particles in batch annealing of Ti stabilised interstitial free steels", ***Materials Science and Technology,*** 20(9): 1192-1198 (2004).

42. Elsen, P., & Hougardy, H. P., "On the mechanism of bake-hardening", ***Steel Research,*** 64(9): 431-436 (1993).

43. Bruce, D. M., Matlock, D. K., Speer, J. G., & De, A. K., "Assessment of the strain-rate dependent tensile properties of automotive sheet steels", ***SAE Technical Paper,*** Canada, 23-55 (2004).

44. Takehide, S., "Physical metallurgy of modern high strength steel sheets", ***ISIJ International,*** 41(6): 520-532 (2001).

45. Gänser, H. P., Werner, E. A., & Fischer, F. D., "Plasticity and ductile fracture of IF steels: experiments and micromechanical modeling", ***International Journal of Plasticity,*** 14(8): 789-803 (1998).

46. Giuliano, G., "Evaluation of the Coulomb friction coefficient in DC05 sheet metal forming", ***Strojniški vestnik-Journal of Mechanical Engineering,*** 61(12): 709-713 (2015).

47. Zhao, H., Rama, S. C., Barber, G. C., Wang, Z. & Wang, X., "Experimental study of deep drawability of hot rolled IF steel", ***Journal of Materials Processing Technology,*** 128(3): 73-79 (2002).

48. He, T., Liu, Y. D., Jiang, Q. W., Wang, G., Wang, Y. D., & Zuo, L., "Microtexture evolution of partially recrystallised interstitial free steel", ***Materials Science and Technology,*** 21(12): 1436-1439 (2005).

49. Vanderschueren, D., Yoshinaga, N., & Koyama, K., "Recrystallisation of Ti IF steel investigated with electron backscattering pattern (EBSP), ***ISIJ International,*** 36(8): 1046-1054 (1996).

50. Suzuki, S., Obata, M., Abiko, K., & Kimura, H., "Effect of carbon on the grain boundary segregation of phosphorus in α-iron", ***Scripta Metallurgica,*** 17(11):

1325-1328 (1983).

51. Yang, G. J., Wang, H. T., Li, C. J., & Li, C. X., "Effect of annealing on the microstructure and erosion performance of cold-sprayed FeAl intermetallic coatings", ***Surface and Coatings Technology,*** 205(24): 5502-5509 (2011).

52. Jin, Y. H., Huh, M. Y., & Chung, Y. H., "Evolution of textures and microstructures in IF-steel sheets during continuous confined strip shearing and subsequent recrystallization annealing", ***Journal of Materials Science,*** 39(16): 5311-5314 (2004).

53. Saray, O., Purcek, G., Karaman, I., Neindorf, T., & Maier, H. J., "Equal-channel angular sheet extrusion of interstitial-free (IF) steel: Microstructural evolution and mechanical properties", ***Materials Science and Engineering: A,*** 528(21): 6573-6583 (2011).

54. Wang, Z., & Wang, X., "A new technology to improve the r-value of interstitial-free (IF) steel sheet", ***Journal of Materials Processing Technology,*** 113(3): 659-661 (2001).

55. Fekete, J. R., "Overview of sheet metals for stamping", ***SAE Transactions,*** Canada, 699-711 (1997).

56. Santecchia, E., Hamouda, A. M. S., Musharavati, F., Zalnezhad, E., Cabibbo, M., & Spigarelli, S., "Wear resistance investigation of titanium nitride-based coatings", ***Ceramics International,*** 41(9): 10349-10379 (2015).

57. Sudharshan, P. Srinivasa, D., Joshi, S. V. and Sundararajan, G. “Effect of process parameters and heat treatments on properties of cold sprayed copper coatings,” ***Journal of Thermal Spray Technology,*** 16(3): 425–434 (2007).

58. Alidokht, S. A., & Chromik, R. R., "Sliding wear behavior of cold-sprayed Ni-WC composite coatings: Influence OF WC content", ***Wear,*** Canada, 203-792 (2021).

59. Villafuerte, J., *"Modern cold spray: materials, process, and applications",* ***Springer,*** Germany, 12-21 (2015).

60. Champagne, V. K., "The cold spray materials deposition process", ***Elsevier Science, Germany,*** 55-63 (2007).

61. Papyrin, A., "The development of the cold spray process", ***Woodhead Publishing,*** UK, 11-42 (2007).

62. Irissou, E., Legoux, J. G., Ryabinin, A. N., Jodoin, B., & Moreau, C., "Review on cold spray process and technology: part I—intellectual property", ***Journal of Thermal Spray Technology,*** 17(4): 495-516 (2008).

63. Grujicic, M., Tong, C., DeRosset, W. S., & Helfritch, D., "Flow analysis and

nozzle-shape optimization for the cold-gas dynamic-spray process", ***Proceedings of the Institution of Mechanical Engineers, Part B: Journal of Engineering Manufacture,*** 217(11): 1603-1613 (2003).

64. Vickers, N. J., "Animal communication: when i'm calling you, will you answer too?", ***Current Biology,*** 27(14): 713-715 (2017).

65. Karthikeyan, J., "The advantages and disadvantages of the cold spray coating process", ***Woodhead Publishing, UK***, 62-71 (2007).

66. Kim, H. J., Lee, C. H. & Hwang, S. Y., "Fabrication of WC–Co coatings by cold spray deposition", ***Surface and Coatings Technology,*** 191(3): 335-340 (2005).

67. Smith, M. F., "Comparing cold spray with thermal spray coating technologies", ***In the cold Spray Materials Deposition Process***, Woodhead Publishing, UK, (pp. 43-61 (2007).

68. Gaydos, S., "Qualification of Cold Spray for Repair of MIL-DTL-83488 Aluminum Coatings (Briefing charts)", ***Boeing Co St Louis Mo.***, USA, 24-31 (2011).

69. Babushkina, E. A., Belokopytova, L. V., Grachev, A. M., Meko, D. M., & Vaganov, E. A., "Variation of the hydrological regime of Bele-Shira closed basin in Southern Siberia and its reflection in the radial growth of Larix sibirica", ***Regional Environmental Change,*** 17(6): 1725-1737 (2017).

70. Wang, H. T., Li, C. J., Yang, G. J., & Li, C. X., "Cold spraying of Fe/Al powder mixture: Coating characteristics and influence of heat treatment on the phase structure", ***Applied Surface Science,*** 255(5): 2538-2544 (2008).

71. Lee, H. Y., Jung, S. H., Lee, S. Y., & Ko, K. H., "Fabrication of cold sprayed Al-intermetallic compounds coatings by post annealing", ***Materials Science and Engineering: A,*** 433(2): 139-143 (2006).

72. Meng, X., Zhang, J., Zhao, J., Liang, Y., & Zhang, Y., "Influence of gas temperature on microstructure and properties of cold spray 304SS coating", ***Journal of Materials Science & Technology,*** 27(9): 809-815 (2011).

73. Dong, S. J., Song, B., Zhou, G. S., Li, C. J., Hansz, B., Liao, H. L., & Coddet, C., "Preparation of aluminum coatings by atmospheric plasma spraying and dry-ice blasting and their corrosion behavior", ***Journal of Thermal Spray Technology,*** 22(7): 1222-1229 (2013).

74. Maev, R. G., & Leshchynsky, V., "Introduction to low pressure gas dynamic spray: physics and technology", ***John Wiley & Sons,*** New York, USA, 60-71 (2009).

75. Chavan, N. M., Kiran, B., Jyothirmayi, A., Phani, P. S., & Sundararajan, G., "The corrosion behavior of cold sprayed zinc coatings on mild steel

substrate", ***Journal of Thermal Spray Technology,*** 22(4): 463-470 (2013).

76. Koivuluoto, H., Coleman, A., Murray, K., Kearns, M., & Vuoristo, P., "High pressure cold sprayed (HPCS) and low pressure cold sprayed (LPCS) coatings prepared from OFHC Cu feedstock: overview from powder characteristics to coating properties", ***Journal of Thermal Spray Technology,*** 21(5): 1065-1075 (2012).

77. Donner, K. R., Gaertner, F., & Klassen, T., "Metallization of thin Al 2 O 3 layers in power electronics using cold gas spraying", ***Journal of Thermal Spray Technology,*** 20(1): 299-306 (2011).

78. Huang, R., & Fukanuma, H., "Study of the influence of particle velocity on adhesive strength of cold spray deposits", ***Journal of Thermal Spray Technology,*** 21(3): 541-549 (2012).

79. Koivuluoto, H., Lagerbom, J., Kylmälahti, M., & Vuoristo, P., "Microstructure and mechanical properties of low-pressure cold-sprayed (LPCS) coatings", ***Journal of Thermal Spray Technology,*** 17(6): 721-727 (2008).

80. Irissou, E., Legoux, J. G., Arsenault, B. & Moreau, C., "Investigation of Al-Al 2 O 3 cold spray coating formation and properties", ***Journal of Thermal Spray Technology,*** 16(6): 661-668 (2007).

81. Lee, H. Y., Jung, S. H., Lee, S. Y., You, Y. H., & Ko, K. H., "Correlation between Al2O3 particles and interface of Al–Al2O3 coatings by cold spray", ***Applied Surface Science,*** 252(5): 1891-1898 (2005).

82. Kubisztal, J., Kubisztal, M., Stach, S., & Haneczok, G., "Corrosion resistance of anodic coatings studied by scanning microscopy and electrochemical methods", ***Surface and Coatings Technology,*** 3(5): 419-427 (2018).

83. Ghelichi, R., MacDonald, D., Bagherifard, S., Jahed, H., Guagliano, M., & Jodoin, B., "Microstructure and fatigue behavior of cold spray coated Al5052", ***Acta Materialia,*** 60(19): 6555-6561 (2012).

84. Villafuerte, J. & Zheng, W., "Corrosion protection of magnesium alloys by cold spray", ***Advanced Materials and Processes,*** 165(9): 53 (2007).

85. Suo, X. K., Guo, X. P., Li, W. Y., Planche, M. P., & Liao, H. L., "Investigation of deposition behavior of cold-sprayed magnesium coating", ***Journal of thermal spray technology,*** *21*(5): 831-837 (2012).

86. Wielage, B., Grund, T., Rupprecht, C., & Kuemmel, S., "New method for producing power electronic circuit boards by cold-gas spraying and investigation of adhesion mechanisms", ***Surface and Coatings Technology,*** 205(4): 1115-1118 (2010).

87. Sova, A., Doubenskaia, M., Grigoriev, S., Okunkova, A., & Smurov, I.,

"Parameters of the gas-powder supersonic jet in cold spraying using a mask, ***Journal of Thermal Spray Technology,*** 22(4): 551-556 (2013).

88. Ning, X. J., Jang, J. H., Kim, H. J., Li, C. J., & Lee, C., "Cold spraying of Al–Sn binary alloy: Coating characteristics and particle bonding features", ***Surface and Coatings Technology,*** 202(9): 1681-1687 (2008).

89. Lee, H., Shin, H., Lee, S., & Ko, K., "Effect of gas pressure on Al coatings by cold gas dynamic spray", ***Materials Letters,*** 62(11): 1579-1581 (2008).

90. Berube, G., Yandouzi, M., Zuniga, A., Ajdelsztajn, L., Villafuerte, J., & Jodoin, B., "Phase stability of Al-5Fe-V-Si coatings produced by cold gas dynamic spray process using rapidly solidified feedstock materials", ***Journal of Thermal Spray Technology,*** 21(2): 240-254 (2012).

91. Koivuluoto, H., & Vuoristo, P., "Effect of powder type and composition on structure and mechanical properties of Cu+ Al 2 O 3 coatings prepared by using low-pressure cold spray process", ***Journal of Thermal Spray Technology,*** 19(5): 1081-1092 (2010).

92. Sova, A., Pervushin, D., & Smurov, I., "Development of multimaterial coatings by cold spray and gas detonation spraying", ***Surface and Coatings Technolo****gy*, 205(4): 1108-1114 (2010).

93. Vickers, N. J., "Animal communication: when i'm calling you, will you answer too?", ***Current Biology,*** *27*(14): 713-715 (2017).

94. Esfahani, E. A., Salimijazi, H., Golozar, M. A., Mostaghimi, J., & Pershin, L., "Study of corrosion behavior of arc sprayed aluminum coating on mild steel", ***Journal of Thermal Spray Technology,*** 21(6): 1195-1202 (2012).

95. Internet: Karthikeyan, J., "Cold spray technology: International status and USA efforts", **http://www.asbindustries.com/do cuments/int_ status_report.pdf/** (2004).

96. Dorfman, M. R., & Sharma, A., "Challenges and strategies for growth of thermal spray markets: the six-pillar plan", ***Journal of Thermal Spray Technology,*** 22(5): 559-563 (2013).

97. Champagne, V. K., & Helfritch, D. J., "A demonstration of the antimicrobial effectiveness of various copper surfaces", ***Journal of Biological Engineering,*** 7(1): 1-7 (2013).

98. Champagne, V. K., "The cold spray materials deposition process", ***Elsevier Science,*** Germany, 67-71 (2007).

99. Davis, J. R., "Handbook of thermal spray technology", **ASM International,** USA, 40-47 (2004).

100. King, P., Yandouzi, M., & Jodoin, B., "The physics of cold spray", ***Modern Cold Spray*, USA,** 31-72 (2015).

101. Kosarev, V. F., Klinkov, S. V., Alkhimov, A. P., & Papyrin, A. N., "On some aspects of gas dynamics of the cold spray process", ***Journal of Thermal Spray Technology*,** 12(2): 265-281 (2003).

102. Papyrin, A., Kosarev, V., Klinkov, S., Alkhimov, A., & Fomin, V. M., "Cold spray technology", ***Elsevier*,** Germany 23-41 (2006).

103. Balani, K., Laha, T., Agarwal, A., Karthikeyan, J., & Munroe, N., "Effect of carrier gases on microstructural and electrochemical behavior of cold-sprayed 1100 aluminum coating", ***Surface and Coatings Technology*,** 195(3): 272-279 (2005).

104. Lemiale, V., King, P. C., Rudman, M., Prakash, M., Cleary, P. W., Jahedi, M. Z., & Gulizia, S., "Temperature and strain rate effects in cold spray investigated by smoothed particle hydrodynamics", ***Surface and Coatings Technology*,** 25(4): 121-130 (2014).

105. Klinkov, S. V., Kosarev, V. F., & Rein, M., "Cold spray deposition: Significance of particle impact phenomena", ***Aerospace Science and Technology*,** 9(7): 582-591 (2005).

106. Murr, L. E., Quinones, S. A., Ayala, A., Valerio, O. L., Hörz, F., & Bernhard, R. P., "The low-velocity-to-hypervelocity penetration transition for impact craters in metal targets", ***Materials Science and Engineering: A*,** 256(2): 166-182 (1998).

107. Schmidt, T., Gärtner, F., Assadi, H., & Kreye, H., "Development of a generalized parameter window for cold spray deposition", ***Acta Materialia*,** 54(3): 729-742 (2006).

108. Fukumoto, M., Terada, H., Mashiko, M., Sato, K., Yamada, M., & Yamaguchi, E., "Deposition of copper fine particle by cold spray process", ***Materials Transactions, Transactions of the Japan Institute of Metals*,** Japan, 749-755 (2009).

109. Ajdelsztajn, L., Schoenung, J. M., Jodoin, B., & Kim, G. E., "Cold spray deposition of nanocrystalline aluminum alloys", ***Metallurgical and Materials Transactions A*,** *36*(3): 657-666 (2005).

110. Spencer, K., & Zhang, M. X., "Heat treatment of cold spray coatings to form intermetallic layers", ***In Materials Forum***, 3(4): 79-84 (2008).

111. DeForce, B. S., Eden, T. J., & Potter, J. K., "Cold spray Al-5% Mg coatings for the corrosion protection of magnesium alloys", ***Journal of Thermal Spray Technology*,** 20(6): 1352-1358 (2011).

112. Schmidt, T., & Assadi, H. and Klassen, T., "From Particle Acceleration to Impact

and Bonding in Cold Spraying", ***J. Therm. Spray Technol,*** 18(6): 794-808 (2009).

113. Wong, W., Rezaeian, A., Irissou, E., Legoux, J. G., & Yue, S., "Cold spray characteristics of commercially pure Ti and Ti-6Al-4V", **In *Advanced Materials Research and Trans Tech Publications Ltd,*** 8(9): 639-644 (2010).

114. Cinca, N., Rebled, J. M., Estradé, S., Peiró, F., Fernández, J., & Guilemany, J. M., "Influence of the particle morphology on the Cold Gas Spray deposition behaviour of titanium on aluminum light alloys", ***Journal of Alloys and Compounds,*** 55(4): 89-96 (2013).

115. Vlcek, J., Gimeno, L., Huber, H., & Lugscheider, E., "A systematic approach to material eligibility for the cold-spray process", ***Journal of Thermal Spray Technology,*** 14(1): 125-133 (2005).

116. Kliemann, J. O., Gutzmann, H., Gärtner, F., Hübner, H., Borchers, C., & Klassen, T., "Formation of cold-sprayed ceramic titanium dioxide layers on metal surfaces", ***Journal of Thermal Spray Technology,*** 20(1): 292-298 (2011).

117. Xu, Y., & Hutchings, I. M., "Cold spray deposition of thermoplastic powder", ***Surface and Coatings Technology,*** 201(6): 3044-3050 (2006).

118. Bu, H., Yandouzi, M., Lu, C., & Jodoin, B., "Post-heat treatment effects on cold-sprayed aluminum coatings on AZ91D magnesium substrates", ***Journal of Thermal Spray Technology,*** 21(3): 731-739 (2012).

119. Kubisztal, J., Kubisztal, M., Stach, S., & Haneczok, G., "Corrosion resistance of anodic coatings studied by scanning microscopy and electrochemical methods", ***Surface and Coatings Technology,*** 3(5): 419-427 (2018).

120. Wolfe, D. E., Eden, T. J., Potter, J. K. & Jaroh, A. P., "Investigation and characterization of Cr 3 C 2-based wear-resistant coatings applied by the cold spray process", ***Journal of Thermal Spray Technology,*** 15(3): 400-412 (2006).

121. Klassen, T., Gärtner, F., Schmidt, T., Kliemann, J. O., Onizawa, K., Donner, K. R., & Kreye, H., "Basic principles and application potentials of cold gas spraying", ***Materialwissenschaft und Werkstofftechnik,*** 41(7): 575-584 (2010).

122. Kang, K., Yoon, S., Ji, Y., & Lee, C., "Oxidation dependency of critical velocity for aluminum feedstock deposition in kinetic spraying process", ***Materials Science and Engineering: A,*** 486(2): 300-307 (2008).

123. Li, C. J., Wang, H. T., Zhang, Q., Yang, G. J., Li, W. Y., & Liao, H. L., "Influence of spray materials and their surface oxidation on the critical velocity in cold spraying", ***Journal of Thermal Spray Technology,*** 19(2): 95-101 (2010).

124. Pawlowski, L., "The science and engineering of thermal spray coatings", ***John Wiley & Sons***, USA, 44-53 (2008).

125. Spencer, K. & Zhang, M. X., "The use of kinetic metallization to form intermetallic reinforced composite coatings by post-spray heat treatment", ***Surface & Coatings Technology,*** 20(203): 3019-3025 (2009).

126. Shrestha, S., Sturgeon, A., Shashkov, P., & Shatrov, A., "Improved Corrosion Performance of AZ91D Magnesium Alloy Coated with the Keronite™ Process", ***In Essential Readings in Magnesium Technology*** Springer**,** Germany, 603-607 (2016).

127. Chiu, L. H., Chen, C. C., & Yang, C. F., "Improvement of corrosion properties in an aluminum-sprayed AZ31 magnesium alloy by a post-hot pressing and anodizing treatment", ***Surface and Coatings Technology,*** 191(2-3): 181-187 (2005).

128. Parco, M., Zhao, L., Zwick, J., Bobzin, K., & Lugscheider, E., "Investigation of HVOF spraying on magnesium alloys", ***Surface and Coatings Technology,*** 201(6): 3269-3274 (2006).

129. Wei, Z. S., Liu, L., & Ding, W. J., "Al arc spray coating on AZ31 Mg alloy and its corrosion behavior", ***In Materials Science Forum and Trans Tech Publications Ltd,*** 48(8): 685-688 (2005).

130. Tsao, C. C., & Chiu, Y. C., "Evaluation of drilling parameters on thrust force in drilling carbon fiber reinforced plastic (CFRP) composite laminates using compound core-special drills", ***International Journal of Machine Tools and Manufacture,*** 51(9): 740-744 (2011).

131. Champagne, V. K. "Repair of magnesium components by cold spray techniques", ***In the Cold Spray Materials Deposition Process***, ***Woodhead Publishing,*** UK, 327-352 (2007).

132. Andreou, A., Knitter, S., Klein, F., Malinka, T., Schmelzle, M., Struecker, B., & Bahra, M., "The role of keratectomy for synchronous liver metastases from pancreatic adenocarcinoma", ***Surgical Oncology,*** 27(4): 688-694 (2018).

133. Winnicki, M., Małachowska, A., Rutkowska-Gorczyca, M., Sokołowski, P., Ambroziak, A., & Pawłowski, L., "Characterization of cermet coatings deposited by low-pressure cold spraying", ***Surface and Coatings Technology,*** 26(8): 108-114 (2015).

134. Yang, T., Yu, M., Chen, H., Li, W. Y., & Liao, H. L., "Characterisation of cold sprayed Al5056/SiCp coating: effect of SiC particle size", ***Surface Engineering,*** 32(9): 641-649 (2016).

135. Wang, Y., Normand, B., Mary, N., Yu, M., & Liao, H., "Effects of ceramic particle size on microstructure and the corrosion behavior of cold sprayed SiCp/Al 5056 composite coatings", ***Surface and Coatings Technology,*** 31(5): 314-325 (2017).

136. McCune, R. C., Donlon, W. T., Popoola, O. O., & Cartwright, E. L., "Characterization of copper layers produced by cold gas-dynamic spraying", ***Journal of Thermal Spray Technology,*** 9(1): 73-82 (2000).

137. Li, W. Y., Li, C. J., Liao, H., & Coddet, C., "Effect of heat treatment on the microstructure and microhardness of cold-sprayed tin bronze coating", ***Applied Surface Science,*** 253(14): 5967-5971 (2007).

138. Meydanoglu, O., Jodoin, B., & Kayali, E. S., "Microstructure, mechanical properties and corrosion performance of 7075 Al matrix ceramic particle reinforced composite coatings produced by the cold gas dynamic spraying process", ***Surface and Coatings Technology,*** 23(5): 108-116 (2013).

139. Popoola, A. P. I., Malatji, N., & Fayomi, O. S. I., "Fabrication and investigation of thermal and wear properties of zinc novel coatings reinforced with nano-al2o3 and cr2o3 particles", ***Archives of Metallurgy and Materials,*** 61(3): 1671–1676 (2016).

140. Hu, H. X., Jiang, S. L., Tao, Y. S., Xiong, T. Y., & Zheng, Y. G., "Cavitation erosion and jet impingement erosion mechanism of cold sprayed Ni–Al2O3 coating", ***Nuclear Engineering and Design,*** 241(12): 4929-4937(2011).

RESUME

Rajab Hussein Rajab ELKILANI graduated primary, elementary, and high school in Misrata city, after that, he started an undergraduate program at High Institute for Comprehensive Professions, Misurata, and was awarded a higher diploma in mechanical engineering in 2011. In February 2014, he graduated from The College of Industrial Technology, Misurata, and awarded a vocational bachelor's degree in the Production and quality control division. Then, in 2019, he started at Karabük University to complete his M. Sc. education.